Search for dark matter production in association with top quarks in the dilepton final state at $\sqrt{s} = 13$ TeV

Afiq Anuar, Alexander Grohsjean, Christian Schwanenberger, Dominic Stafford, Nicole Stefanov (1), Kristian Hahn, Kevin Sung (2), Pablo Martinez Ruiz Del Arbol, Jónatan Piedra, **Cédric Prieels (3)**, Deborah Pinna, Victor Shang (4)

March 18th 2021

(1) DESY
(2) NorthWestern University
(3) Instituto de Fisica de Cantabria
(4) University of Wisconsin

Focus of this analysis I

We are searching for dark matter produced in association with either one or two top quarks. Several **simplified models** are interesting to consider:

- Spin 1/2 DM χ ($\in [1, 55]$ GeV, Dirac fermion)
- Spin 0 scalar (S)/pseudoscalar (PS) mediator ϕ/a (Yukawa-like structure of such interactions $\rightarrow$ gain from the coupling of the mediator to top quarks)
- Mediator mass $\in [10, 1000]$ GeV
- Coupling g_χ mediator/DM set to 1 (same for all g_q couplings)

$t/\bar{t}$+DM tW models

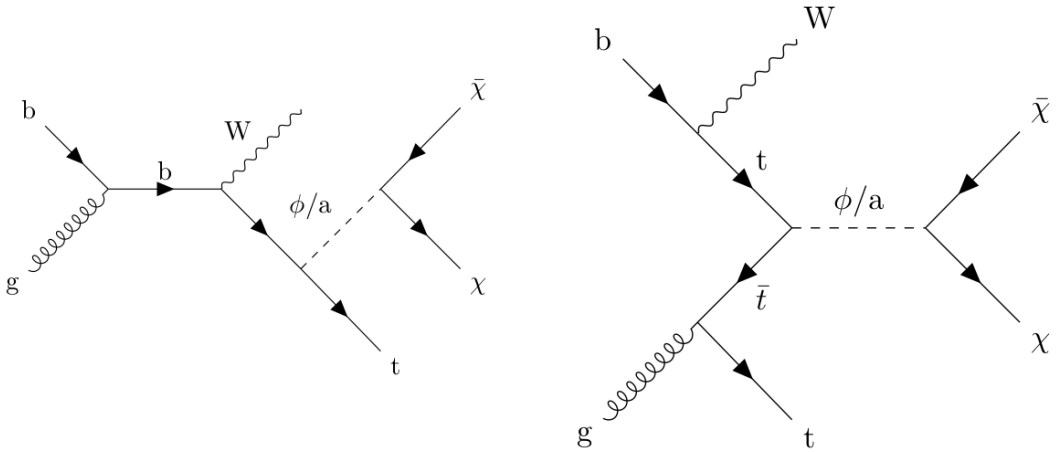

$t\bar{t}$+DM model

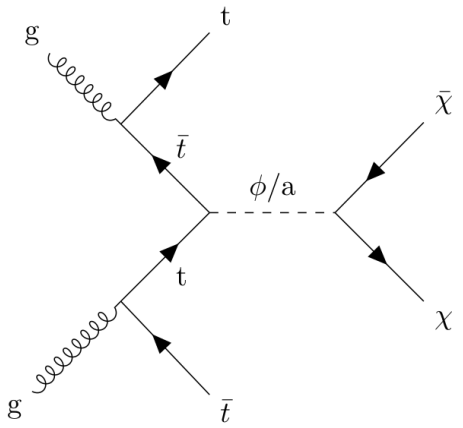

Focus of this analysis II

The **typical final state** of such models is made out of:

- 1 or 2 b-tagged jets coming from the decay of the top quark(s);
- 2 W bosons, seen as a combination of jets and leptons depending on the channel;
- Some MET coming from the dark matter and the decay of the Ws;

In particular, we are studying the dilepton final state in this work:

- Has the lowest branching ratio: $\mathrm{BR}(W \to l^+ + \nu_l) = (10.80 \pm 0.09)\%$ for each of the tree leptons (contains only 5% of the signal events);
- But, leptons can usually be reconstructed better than jets, resulting in lower systematic uncertainties;
- And this channel also has the lowest number of backgrounds, resulting in a better signal isolation.

This channel is then **expected to be competitive with the hadronic channel**, especially when considering high mediator masses, which feature a higher global discrimination signal/background.

Run II legacy paper being worked on, expected to combine both the $t/\bar{t}$+DM and $t\bar{t}$+DM searches, and the 3 possible final states (hadronic, semi-leptonic and dileptonic).
$\rightarrow$ Paper expected to be approved by LHCP ($\sim$ June).

The effort is **globally common** between the groups studying the different final states:

- Objects are defined in a common way;
- Control and signal region orthogonal between the channels.
  - Number of leptons and b-jet categorization to improve the sensitivity by defining enriched $t/\bar{t}$+DM/$t\bar{t}$+DM regions.

This talk will **be focused on the dilepton final state**, in which we are mostly involved, along with a team of DESY. Deborah Pinna and her team from the University of Wisconsin are focused on the semi-leptonic and hadronic channels.

This analysis **almost entirely relies on the Latino framework**:

- We use the usual Latino objects;
- We produced our own signal trees privately, stored in our own eos directories given the tight space available in the HWW directory;
- A custom post-processing step was run on top of the l2tight trees, in order to:
  - Perform a general Betchart reconstruction of the $t\bar{t}$ system;
  - Skim the trees;
  - Compute and store additional variables, such as the number o medium deepCSV b-jets or the stranverse mass m_{T2}^{ll} as used in EXO.

A custom setup made in PlotsConfigurations was then used to plot the results and produce the datacards needed.

In general, the process was really smooth given the reliability of the framework in general and the high number of scripts available, able to perform a lot of different taks.

Inclusive selection

Inclusive selection

First, distributions in the following inclusive control region mostly enriched in Drell-Yan were studied, in all the different channels available:

- Leading (trailing) lepton $p_T > 25$ (20) GeV
- Third lepton veto ($p_T < 10$ GeV)
- Opposite sign leptons
- $m_{ll} > 20$ GeV to avoid low mass resonances
- At least 1 jet
- At least 1 medium deep CSV b-jet

This region is studied to have a look at the most inclusive selection to spot initial issues and problems.

A slight mismodeling of the low mass DY+Jets sample and a general problem of the MET in DY events is observed, but these features are known in CMS and are mitigated with the analysis cuts applied.

Inclusive control region

// channel

2016

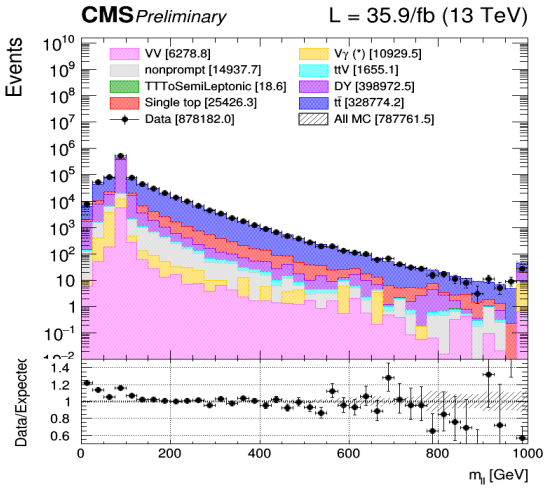

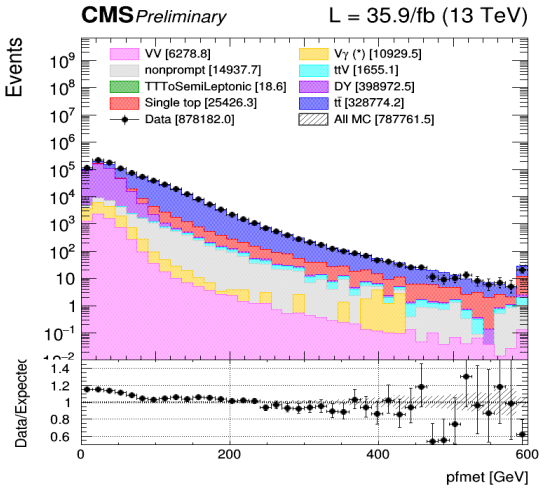

2017

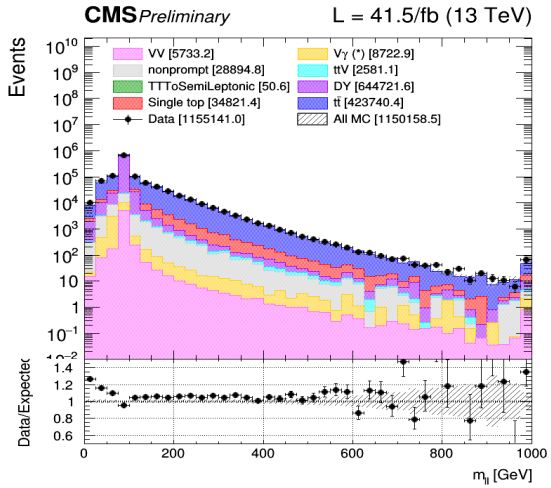

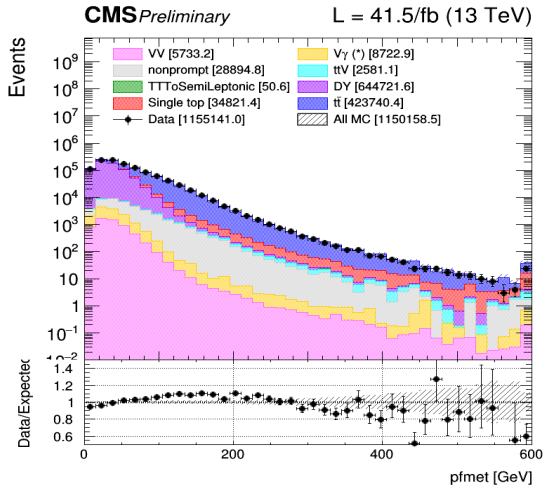

2018

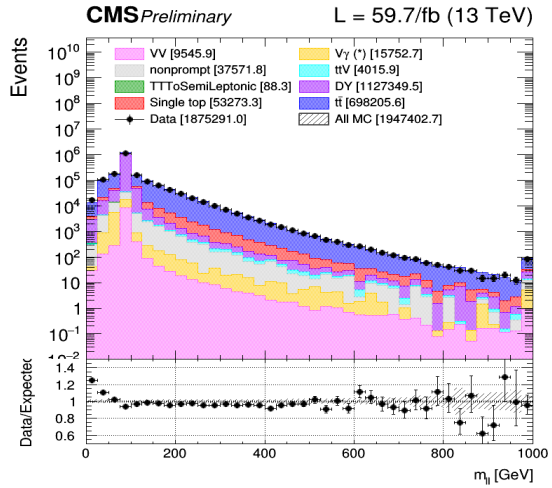

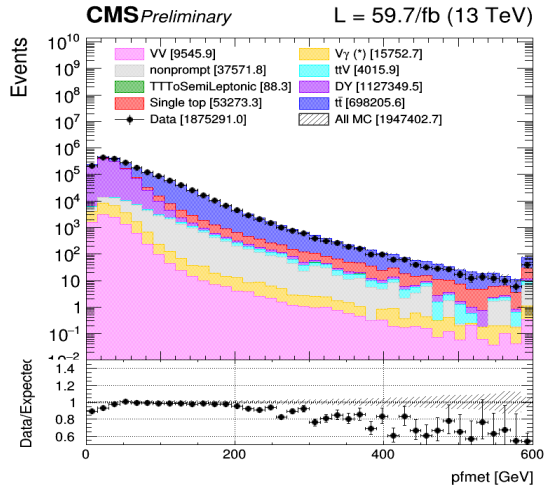

Inclusive control region

df channel

2016

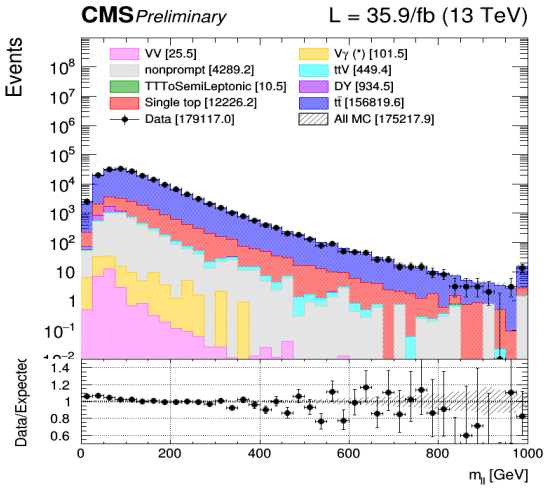

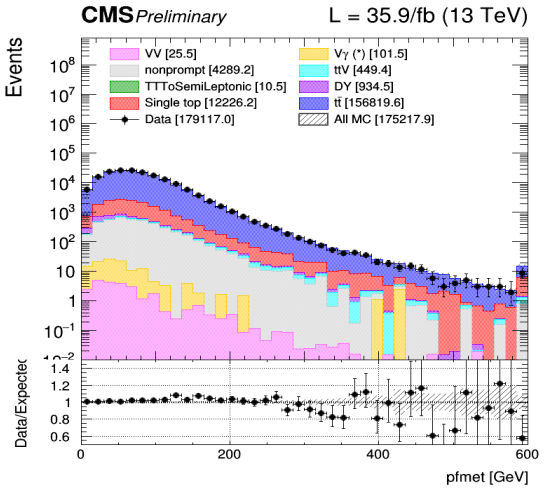

2017

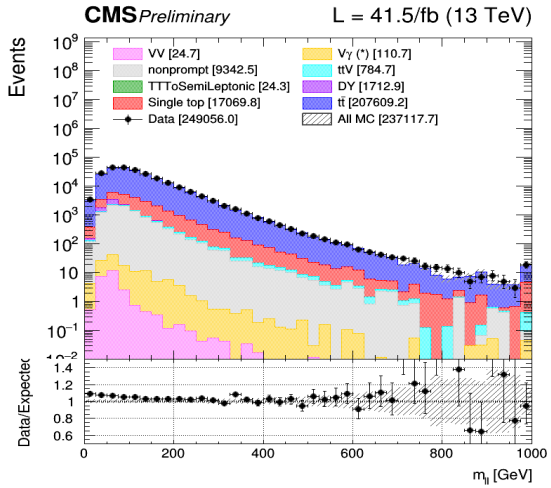

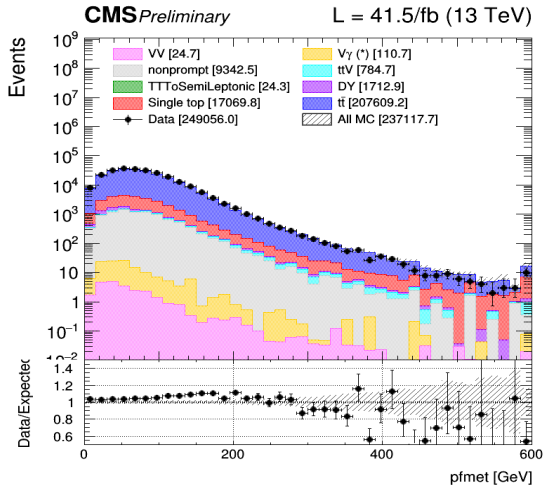

2018

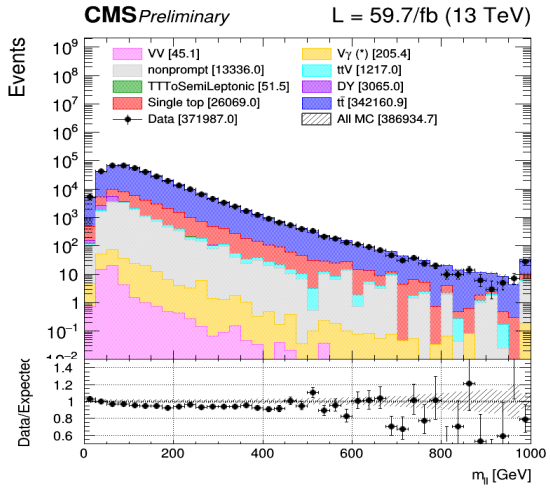

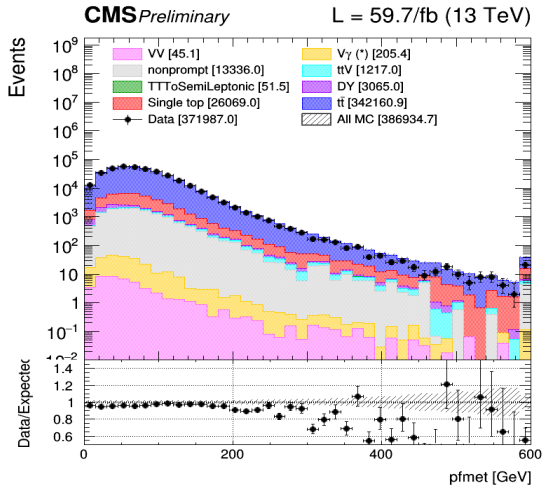

Signal extraction

We trained an ANN, featuring the following characteristics:

- 80/80/40 hidden neurons
- Mix of standard model $t\bar{t}$ and single top as **backgrounds**, and mix of both $t/\bar{t}$+DM and $t\bar{t}$+DM as **signals**;
- Only events passing the **following pre-selection** are considered for the training:
  - 2 tight leptons: $p_T > 25, 20$ GeV
  - Third lepton: $p_T < 10$ GeV
  - Opposite sign leptons
  - $m_{ll} > 20$ GeV
  - 15 GeV Z-veto in ee and $\mu\mu$ channels
  - At least 1 jet
  - At least 1 b-jet
  - $M_{T2}^{ll} > 80$ GeV, to stay orthogonal to the other channels
- One specific training performed per signal mass point;
- 50% train/test splitting used ($\sim$ 40.000 training events in total).

The ANN shape obtained is used to perform a general shape analysis.

The TMVA package was then finally used to study the training performed, as shown in the next few slides for the 2016 scalar 100/500GeV training performed. We plan on combining all the year together.

2018 discriminating variables

Example distributions shown in the blinded 2018 pre-selection region.

2018, // channel

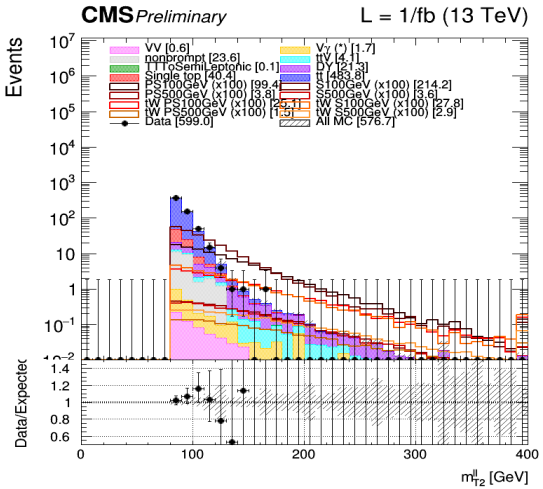

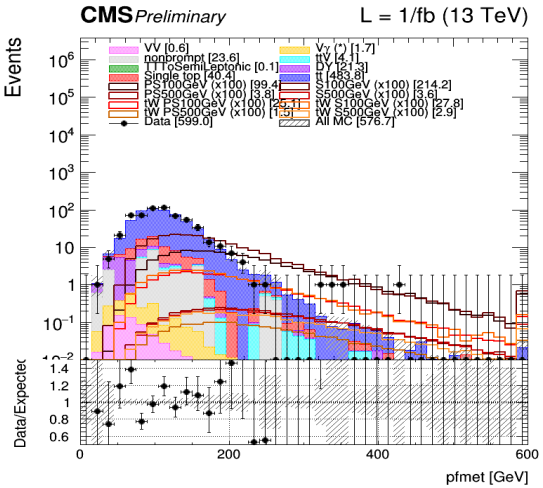

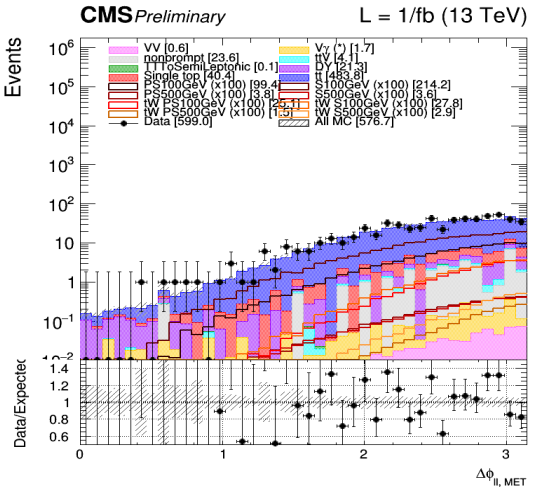

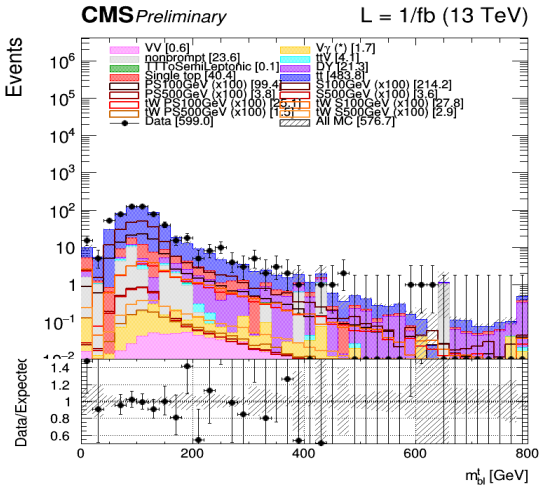

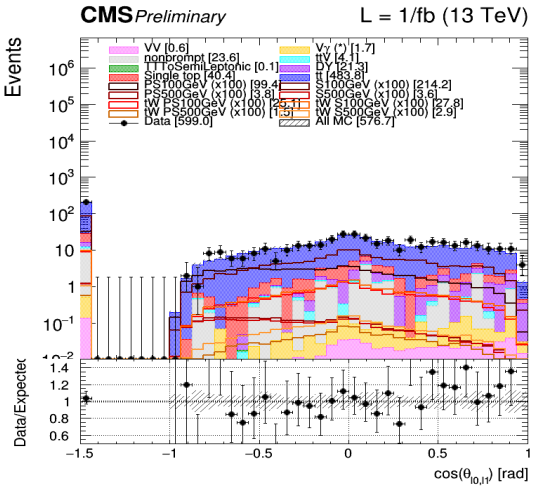

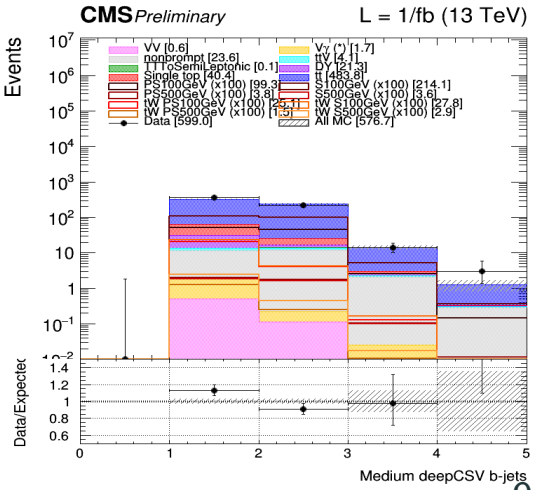

ROC curves have been obtained for all the different mass points available, from 50 to 500 GeV, and for both scalar and pseudoscalar mediators.

Scalar mediator

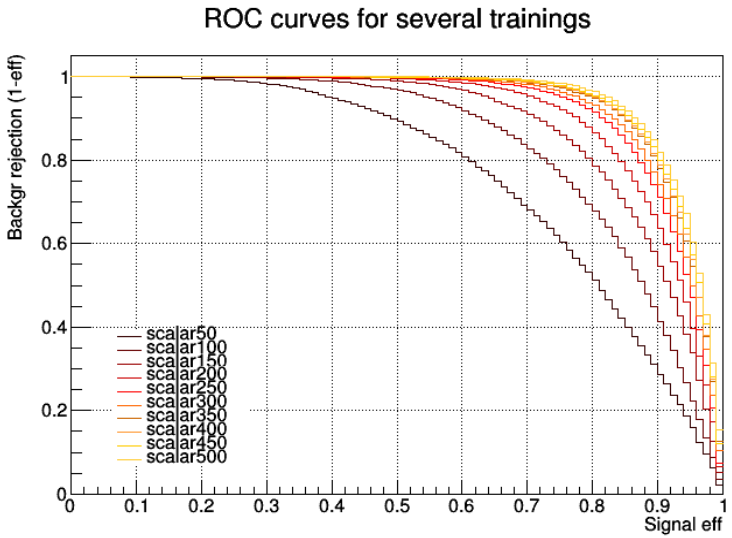

Pseudoscalar mediator

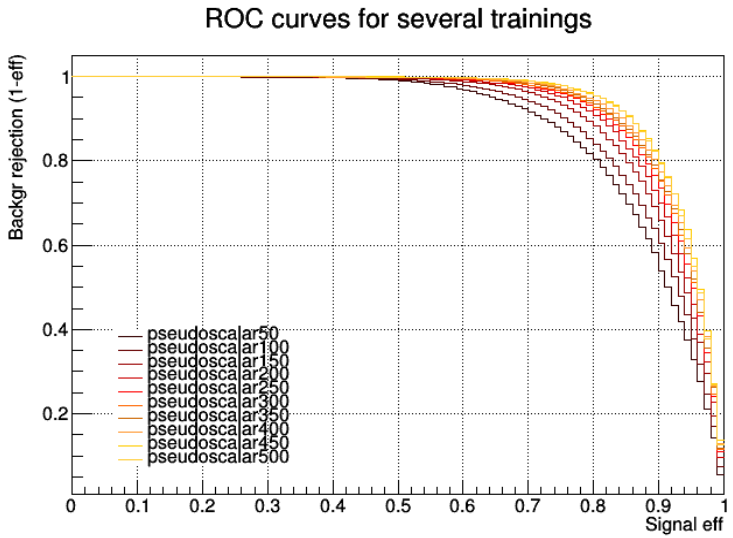

As expected, a better discrimination is achieved for higher mediator masses.

Blinded ANN output shape

Scalar 100 GeV output shape

2016

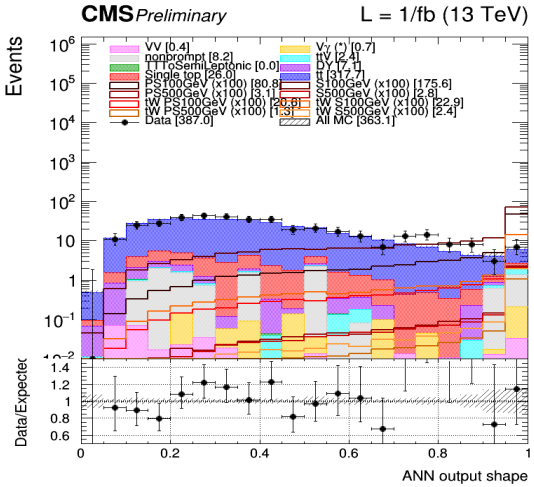

2017

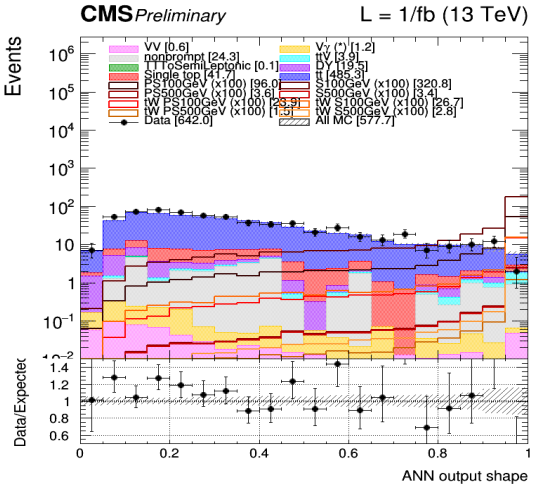

2018

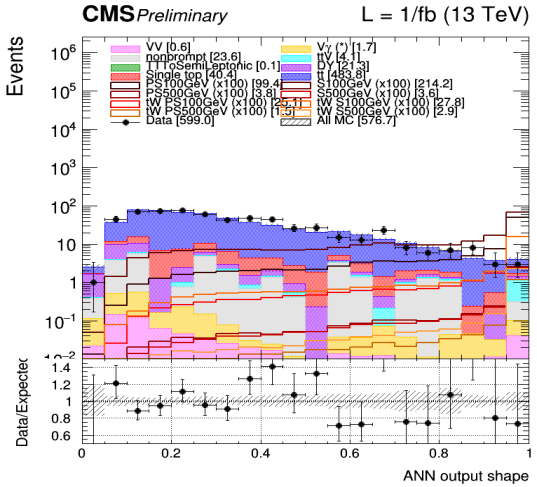

Scalar 500 GeV output shape

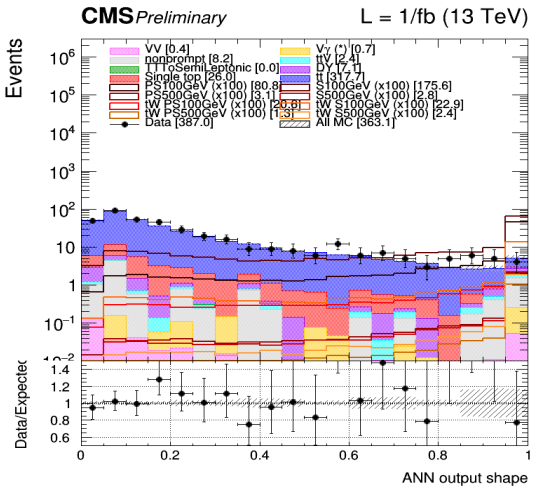

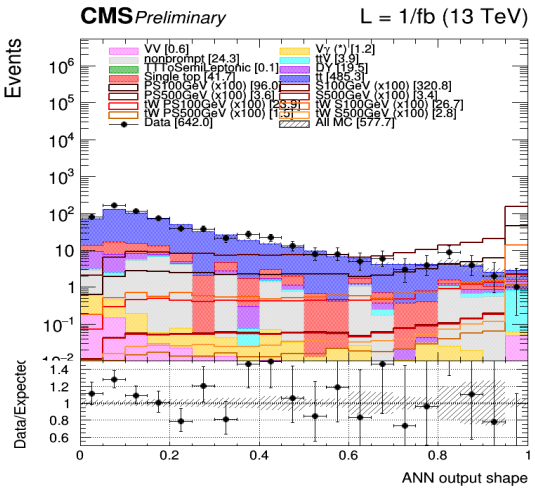

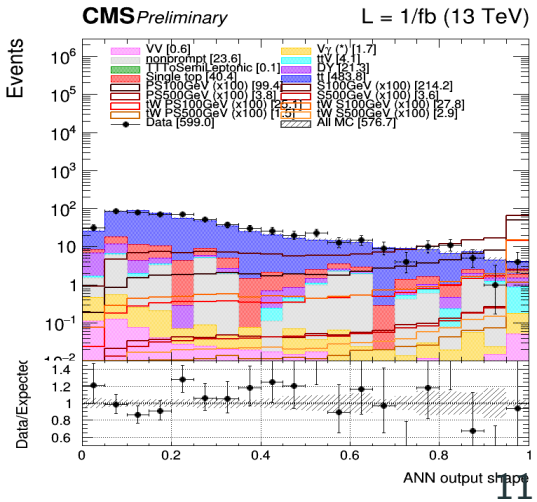

Background prediction methods

The backgrounds are predicted either directly from Monte-Carlo simulations or from data-driven methods. In order of importance:

- The $t\bar{t}$ **and the single top** are taken from simulation accounting for all the variations in the generation parameters. Several parameters (QCD scale, PDF variation,...) are varied and included as a systematic (see later).
  $\rightarrow$ A data validation region (low M_{T2}^{ll}) is explored to ensure the quality of the prediction;
- The **Drell-Yan** yields are obtained from a semi data-driven method using the excluded same flavor region on the Z peak as control region;
- The **non-prompt contamination** is estimated from data control regions and validated in a same sign validation region;
- The irreducible **ttV process** (ttW + ttZ) is taken from simulation and checked in a particular validation region;
- **Diboson processes and other minor backgrounds** are taken directly from MC.

Top control region

Same as the signal region but with $60 < M_{T2}^{ll} < 80$ GeV.

// channel

2016

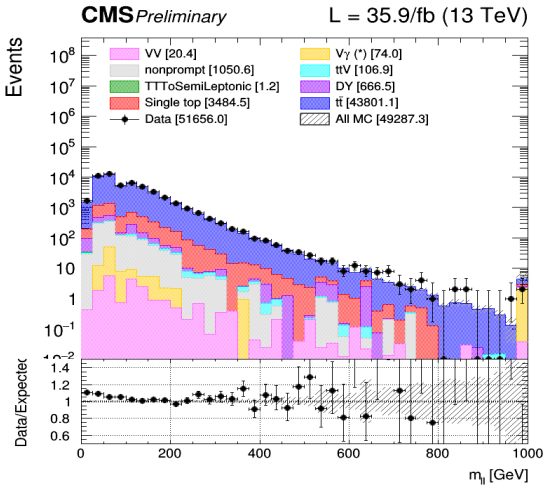

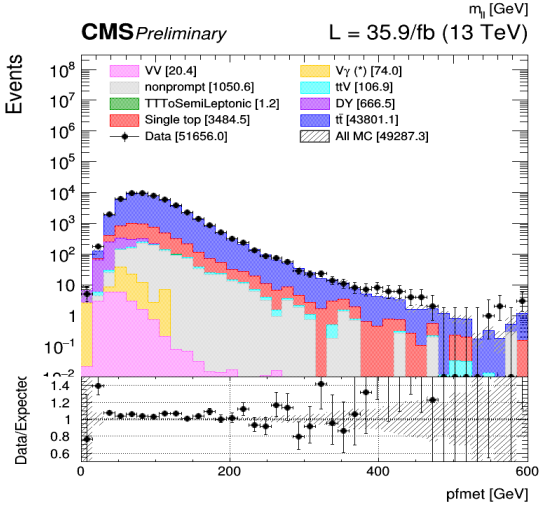

2017

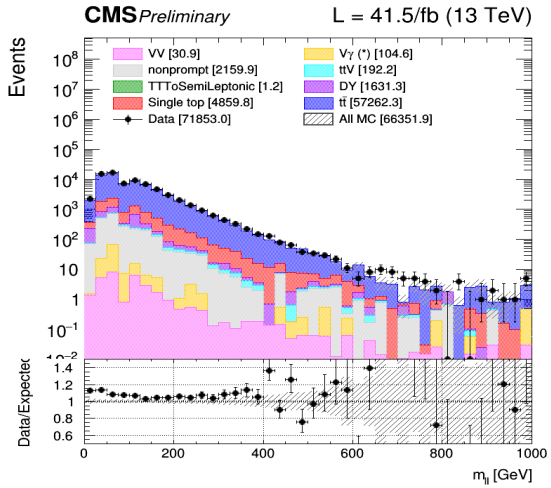

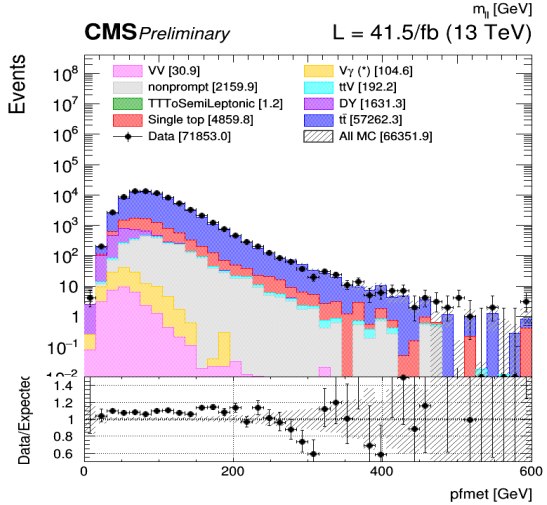

2018

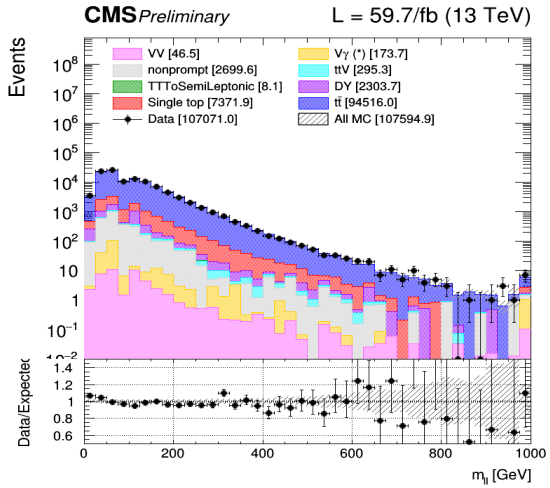

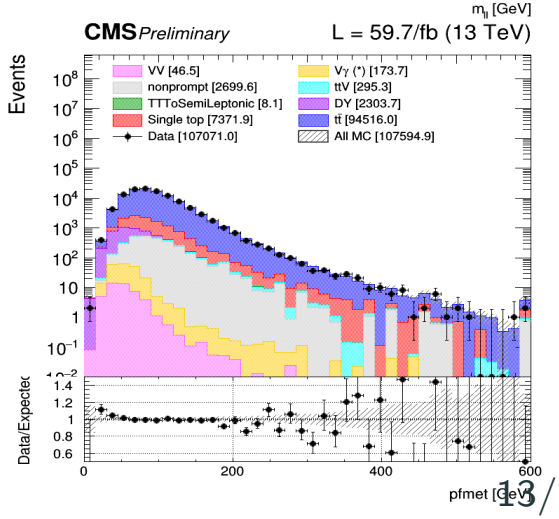

We want to **estimate the DY yields outside of the Z-peak from the data**:

- Given the presence of large backgrounds (such as $t\bar{t}$) in the analysis region, we go inside of the Z-peak to compute the Rin-out factor:

$$N_{DY}^{out} = N_{DY,data}^{in} \cdot \kappa \cdot \left(\frac{N_{DY,MC}^{out}}{N_{DY,MC}^{in}} \right) \equiv N_{DY,data}^{in} \cdot \frac{R_{out/in,\ MC}^{0bj}}{R_{out/in,\ data}^{0bj}} \cdot R_{out/in,\ MC}$$

- To avoid any bias, the contamination of non-peaking backgrounds is removed and we correct this factor by the ratio κ between the data/MC transfer factors in a CR close to the SR (asking for 0 b-jet instead of 1);
- We then get this Rin-out in **bins of MET and for each channel (ee, $\mu\mu$) separately**:

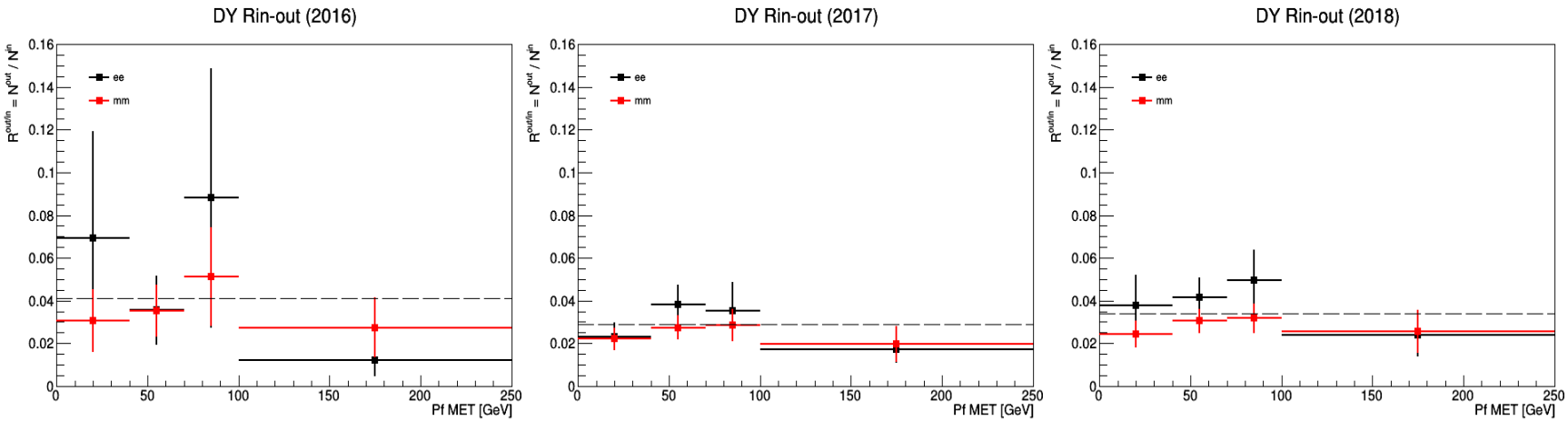

A flat scale factor and a fixed 20% systematic uncertainty is then applied to the DY. This method and the difference in statistics are still being studied.

DY control region

// channel

2016

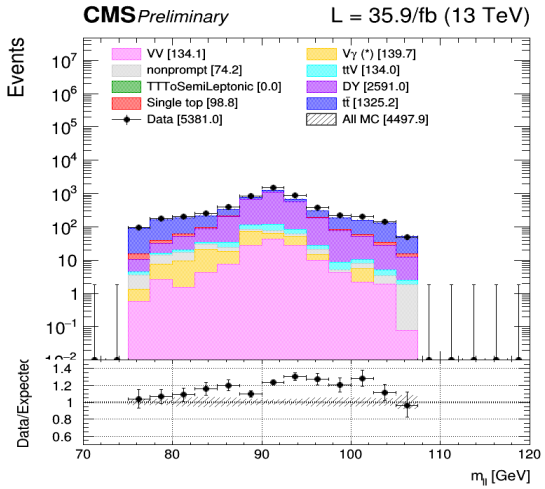

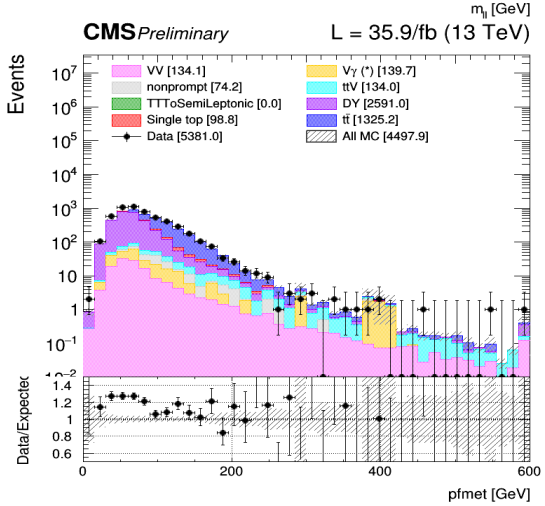

2017

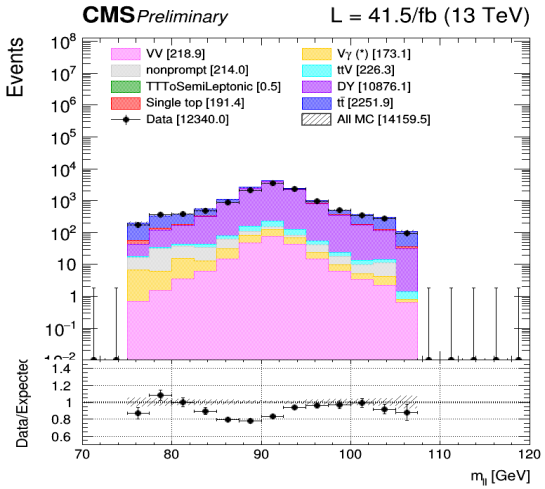

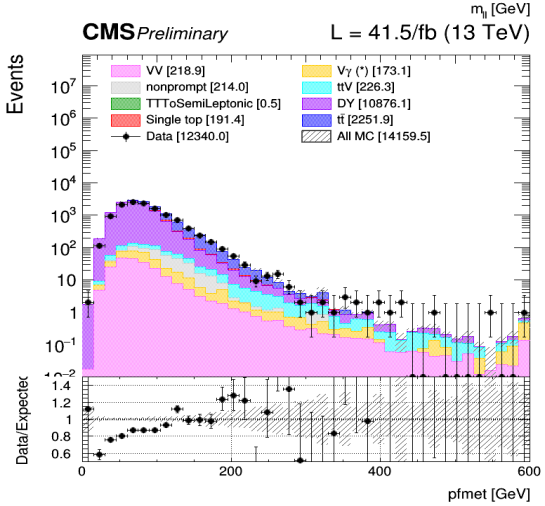

2018

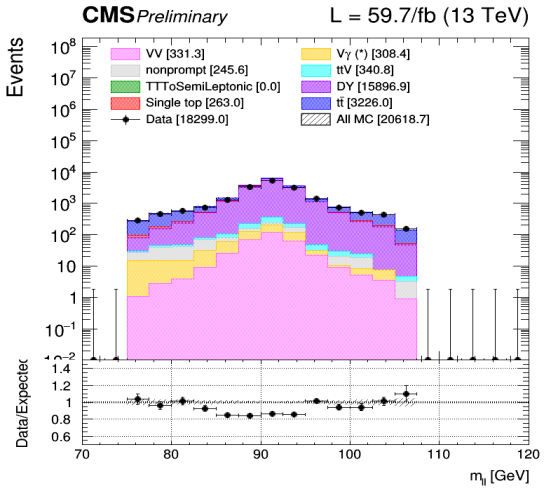

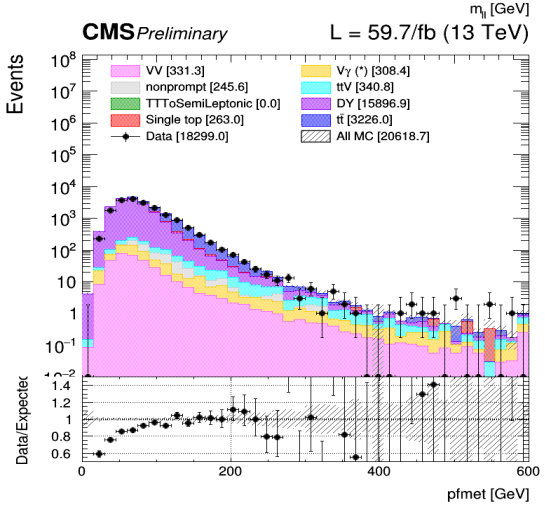

The 0-bjet correction allows us to fix the data/MC discrepancies observed. A large systematic uncertainty is associated to this background, minor in the signal regions.

Fake leptons detection (mostly jets misidentified or leptons coming from semileptonic b-quark decays $b \to cW \to cl\nu$) in the detector needs to be taken into account, through a data-driven tight-to-loose method since the Monte-Carlo is not reliable in this case:

Fake rate

- A QCD enriched region is defined with a looser particle selection criteria, where the misidentification should be high;
- Any eventual contamination from electroweak processes in this region is removed;
- The fake rate is defined as the ratio between the fakeable object (lepton-like objects passing only the loose isolation requirements) and fully selected objects yields.

Prompt rate

- The prompt rate, taking into account the real lepton contamination is calculated in a Z enriched region from a general tag and probe method.

Then, we calculate from data an extrapolation factor to go back to the signal region of the analysis and the results obtained are checked in a same sign control region.

Non-prompt contamination II

2016 fake rate

Electron

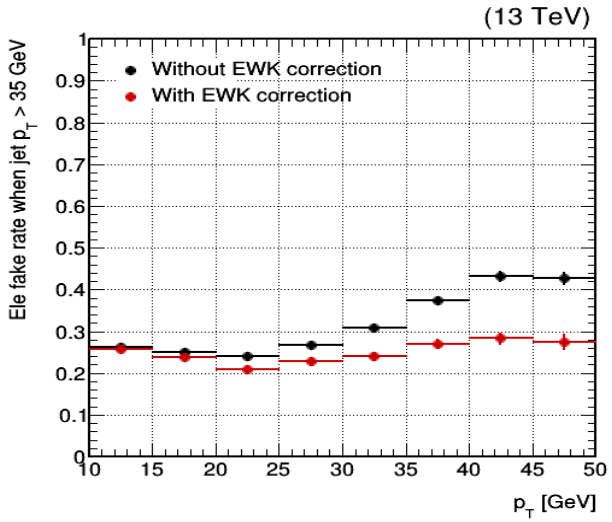

Muon

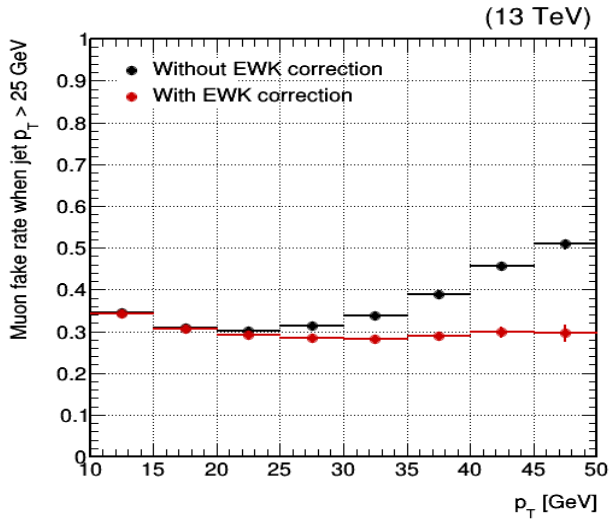

2016 prompt rate

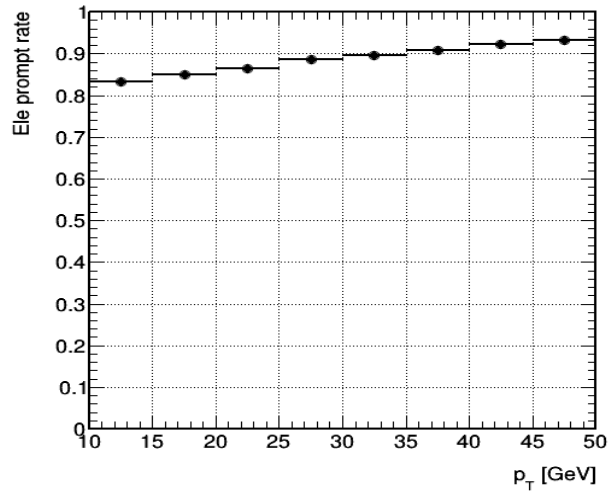

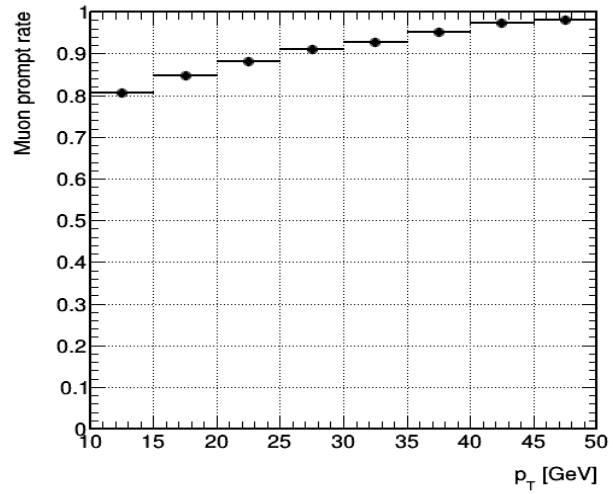

Same sign control region

This is checked in a dedicated same sign control region.

// channel

2016

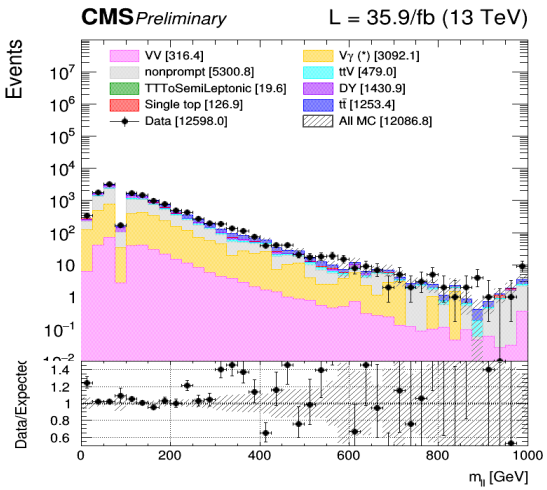

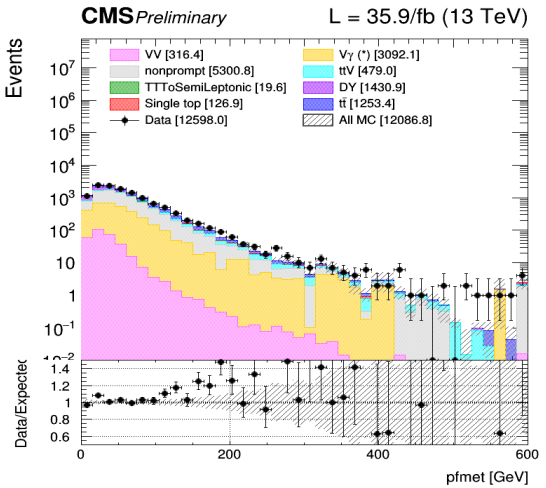

2017

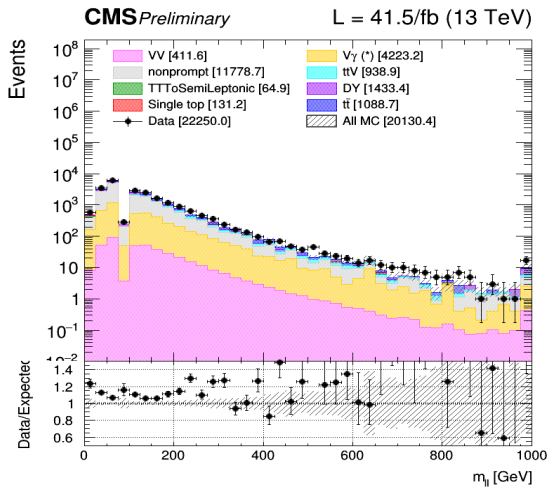

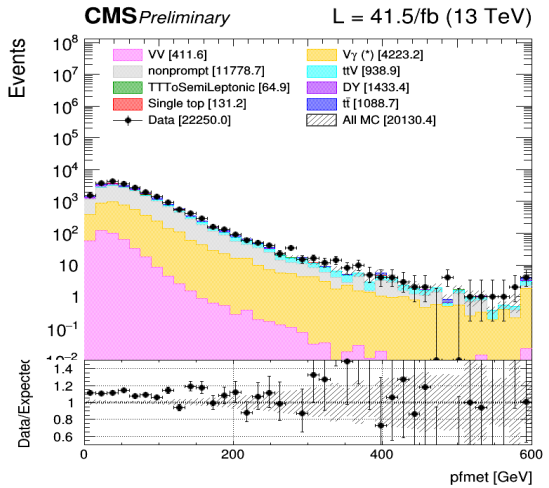

2018

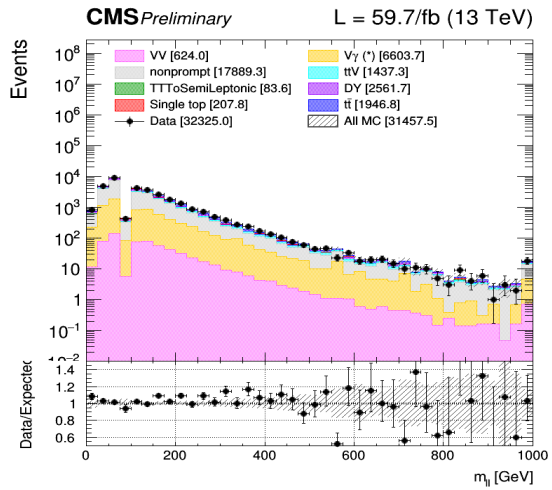

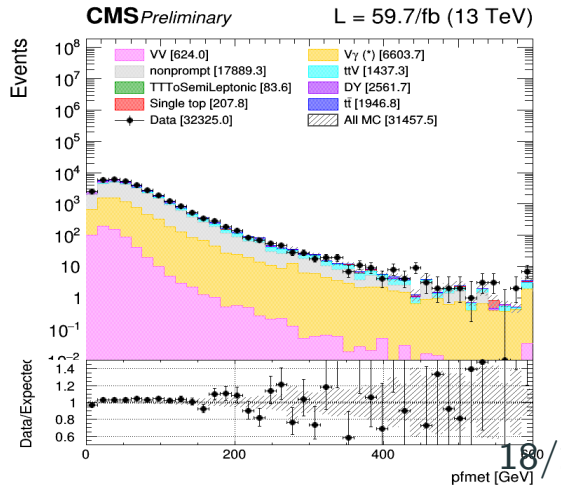

This process is taken directly from MC, and crosschecked in a dedicated control region.

// channel

2016

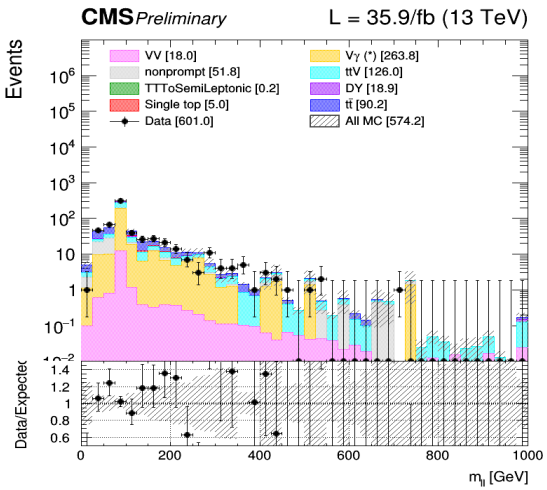

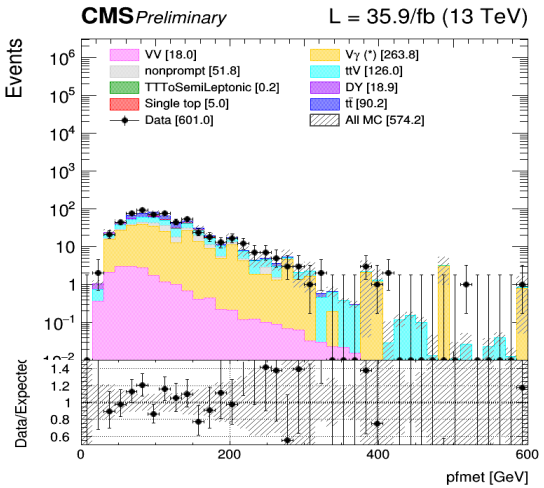

2017

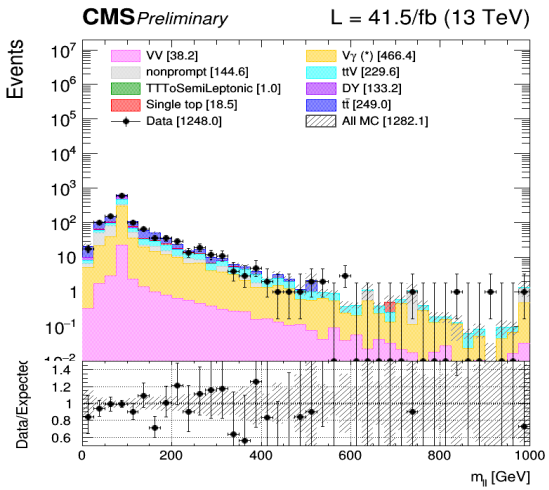

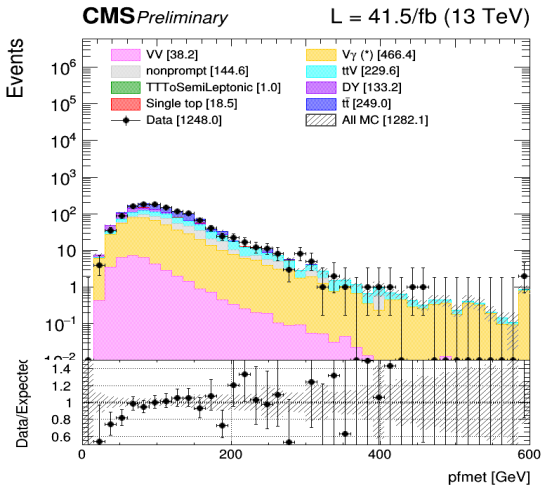

2018

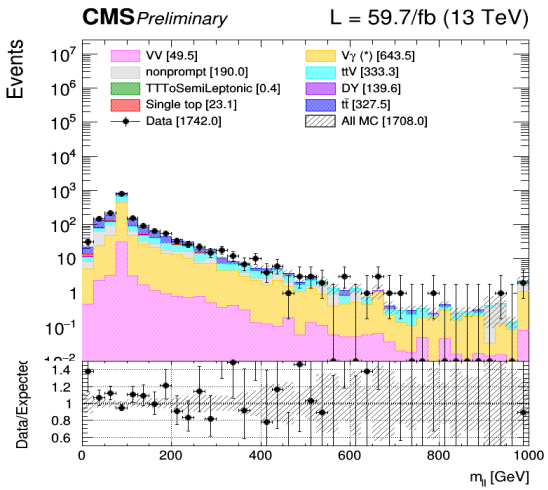

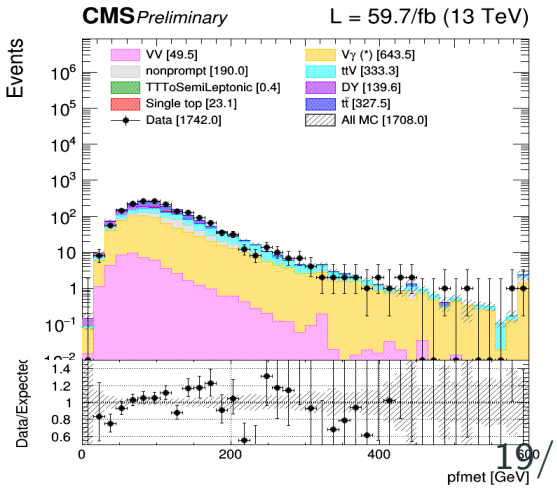

Systematic uncertainties

Systematic uncertainties

Most of the systematics to be considered (on top of the statistical uncertainties) are already in place, such as:

Theoretical uncertainties

- PDF and higher order corrections, underlying event and parton shower, renormalization and factorization scales.

Experimental uncertainties

- Luminosity, pileup modeling, lepton trigger, lepton efficiency and energy scale, jet energy scale, MET mismodelling, b-tagging efficiency, top p_T reweighting.

Background specific uncertainties

- Drell-Yan and non-prompt backgrounds related uncertainties.

Disclaimer: this part of the analysis still needs to be checked/optimized, so results shown next are preliminary and expected to change in the future.

Results obtained

Scalar upper limits

2016

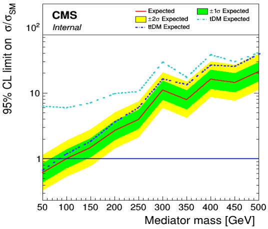

2017

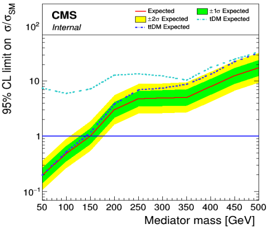

2018

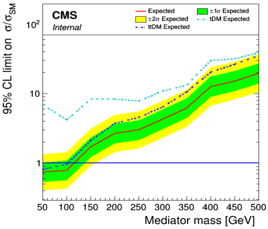

Pseudoscalar upper limits

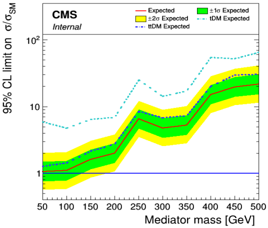

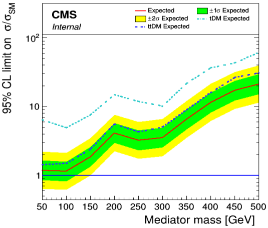

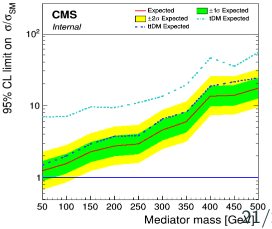

Disclaimer: preliminary comparison done with some systematics missing, so results are expected to change a bit.

Scalar mediators

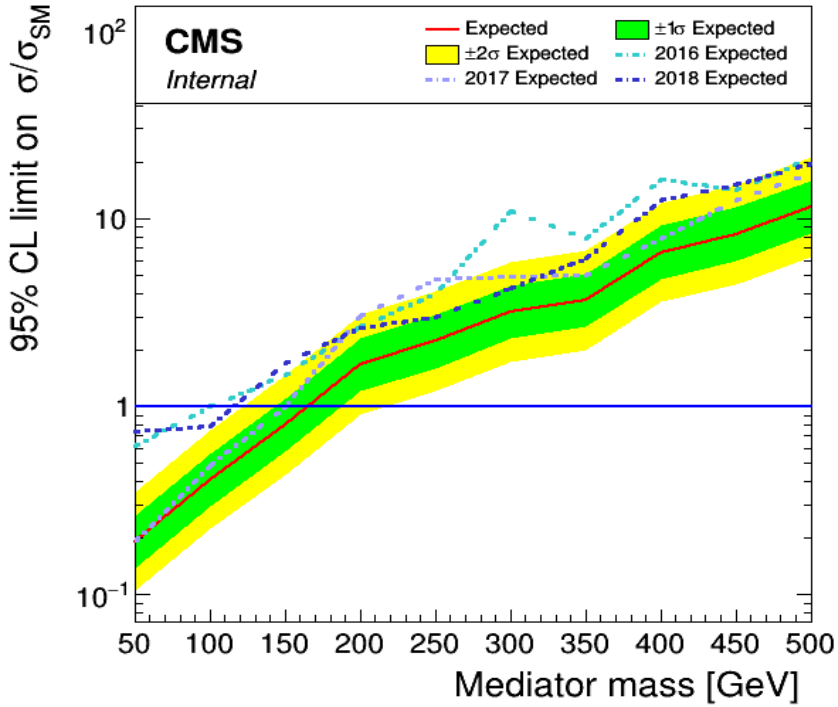

Pseudoscalar mediators

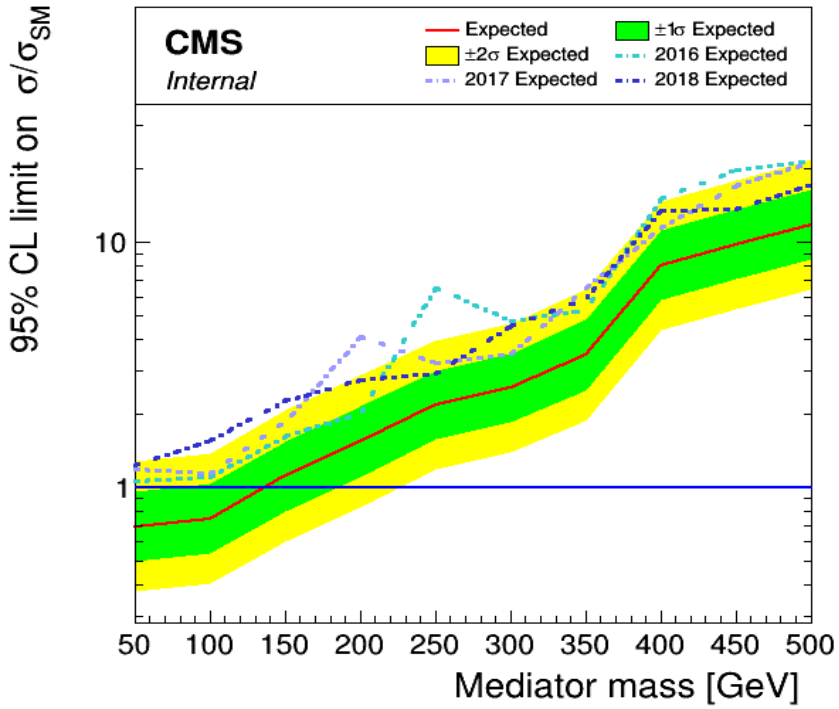

A search for dark matter produced in association with either one or two top quarks is on-going using the Latino framework:

- This search is considering the **Run II legacy dataset** collected by the CMS detector;
- At IFCA, our efforts are entirely focused on the **dilepton final state**;
- This search is performed by defining a ANN, training it to be able to recognize background and signal events, to separate them and **increase the signal efficiency**;
- First time that such a combination will be performed considering this canal, which should increase by a lot the limits published in 2016;
- We expect this analysis to be approved by June.

In general, using the Latino framework was extremely helpful given its reliability and global ease of use.

Back up

CMS dilepton channel 2016 results published:

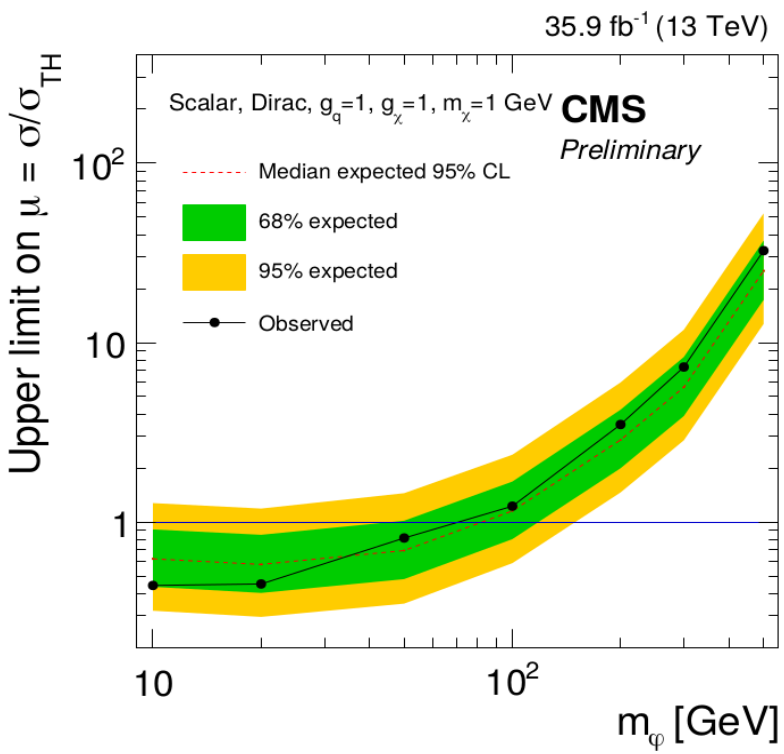

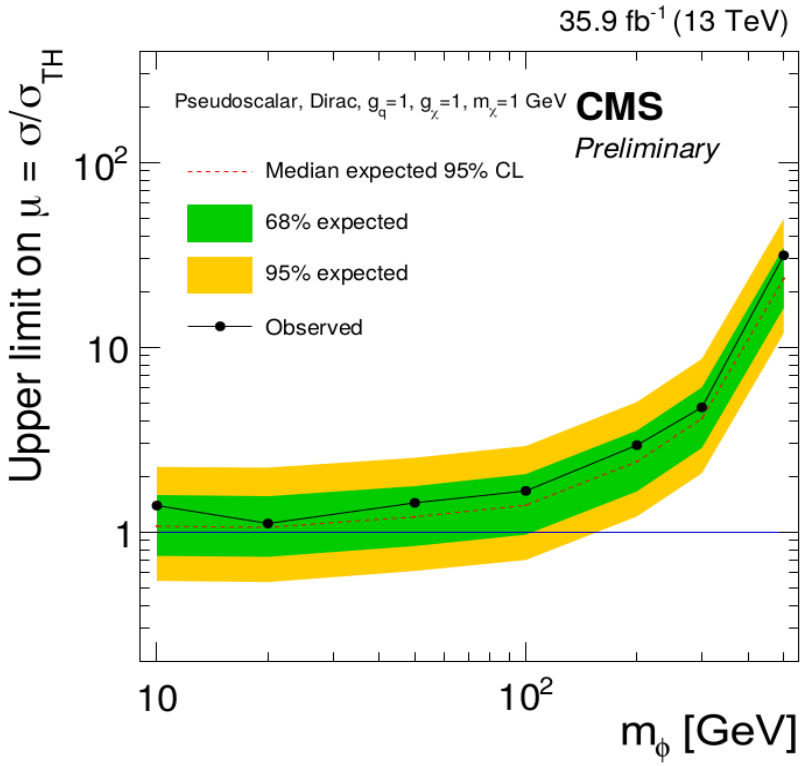

A **combination** of both the $t/\bar{t}$+DM and $t\bar{t}$+DM processes has also been performed.

The inclusion of the single top signal process improved up to a factor 2 the limits obtained by the $t\bar{t}$ analysis on its own. This analysis:

- Only considered the 2016 data-taking period;
- And only considered the semi-leptonic and hadronic final states.

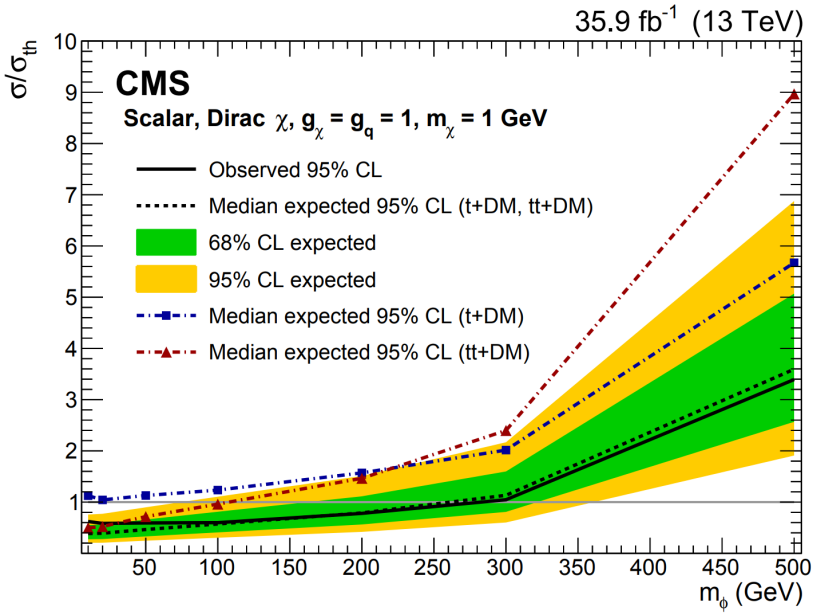

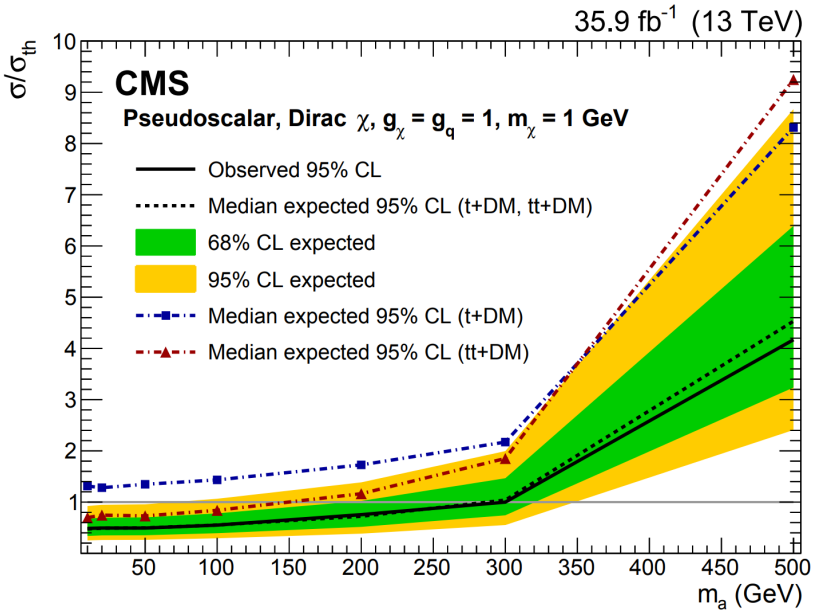

Scalar (pseudoscalar) mediators were with this combination excluded up to 290 (300) GeV at the 95% confidence level.

ATLAS dilepton channel Run II legacy resuts from ICHEP 2020:

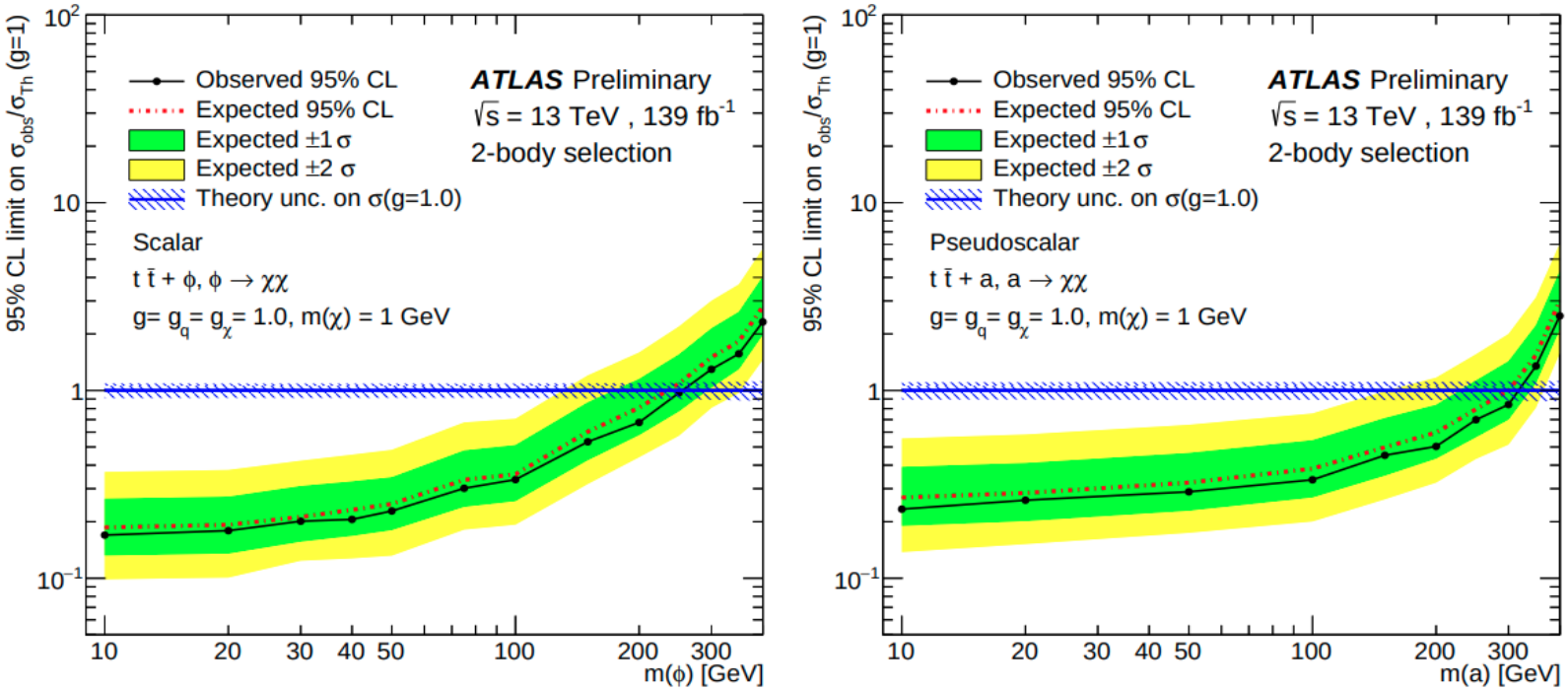

The ATLAS collaboration does not perform any combination between the different channels though.

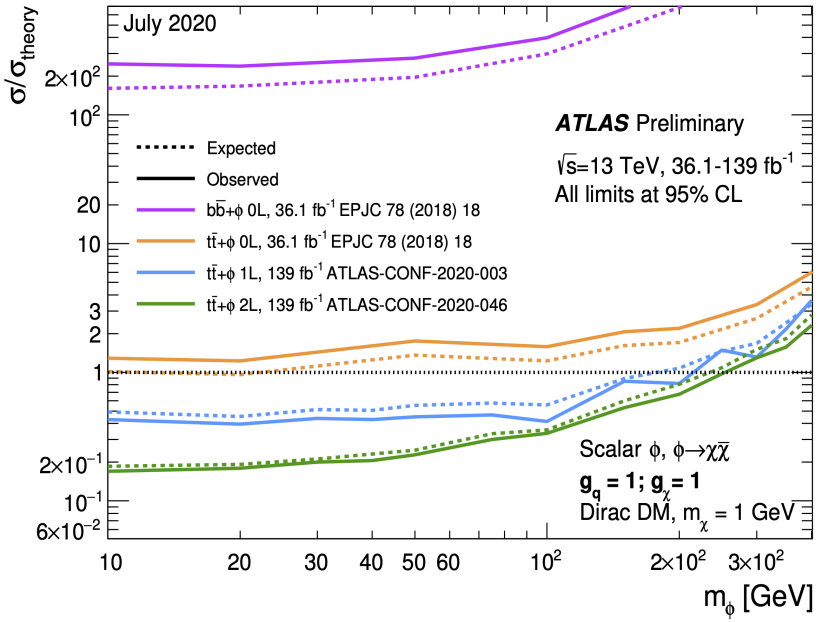

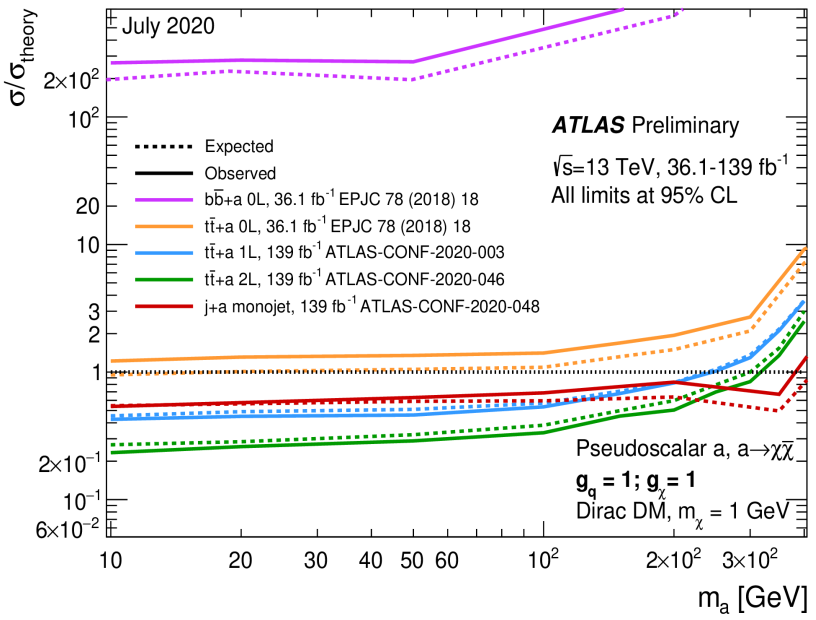

2016 data samples

Dataset	Events (size)	$\mathcal{L}$ [fb^{-1}]
Run 2016B		
/DoubleEG/Run2016B_ver2-Nano02Apr2020_ver2-v1/NANOAOD	143073268 (99.4Gb)	
/DoubleMuon/Run2016B_ver2-Nano02Apr2020_ver2-v1/NANOAOD	82535526 (53.2Gb)	
/MuonEG/Run2016B_ver2-Nano02Apr2020_ver2-v1/NANOAOD	32727796 (26.8Gb)	5.8
/SingleElectron/Run2016B_ver2-Nano02Apr2020_ver2-v1/NANOAOD	246440440 (167.8Gb)	
/SingleMuon/Run2016B_ver2-Nano02Apr2020_ver2-v1/NANOAOD	158145722 (96.4Gb)	
Run 2016C		
/DoubleEG/Run2016C-Nano02Apr2020-v1/NANOAOD	47677856 (35.3Gb)	
/DoubleMuon/Run2016C-Nano02Apr2020-v1/NANOAOD	27934629 (19.7Gb)	
/MuonEG/Run2016C-Nano02Apr2020-v1/NANOAOD	15405678 (12.8Gb)	2.6
/SingleElectron/Run2016C-Nano02Apr2020-v1/NANOAOD	97259854 (69.3Gb)	
/SingleMuon/Run2016C-Nano02Apr2020-v1/NANOAOD	67441308 (42.4Gb)	
Run 2016D		
/DoubleEG/Run2016D-Nano02Apr2020-v1/NANOAOD	53324960 (39.6Gb)	
/DoubleMuon/Run2016D-Nano02Apr2020-v1/NANOAOD	33861745 (24.1Gb)	
/MuonEG/Run2016D-Nano02Apr2020-v1/NANOAOD	23482352 (19.4Gb)	4.2
/SingleElectron/Run2016D-Nano02Apr2020-v1/NANOAOD	148167727 (104.4Gb)	
/SingleMuon/Run2016D-Nano02Apr2020-v1/NANOAOD	98017996 (61.3Gb)	
Run 2016E		
/DoubleEG/Run2016E-Nano02Apr2020-v1/NANOAOD	49877710 (37.9Gb)	
/DoubleMuon/Run2016E-Nano02Apr2020-v1/NANOAOD	28246946 (20.8Gb)	
/MuonEG/Run2016E-Nano02Apr2020-v2/NANOAOD	22519303 (19.0Gb)	4.0
/SingleElectron/Run2016E-Nano02Apr2020-v1/NANOAOD	117321545 (86.5Gb)	
/SingleMuon/Run2016E-Nano02Apr2020-v1/NANOAOD	90984718 (58.7Gb)	
Run 2016F		
/DoubleEG/Run2016F-Nano02Apr2020-v1/NANOAOD	34577629 (26.9Gb)	
/DoubleMuon/Run2016F-Nano02Apr2020-v1/NANOAOD	20329921 (15.3Gb)	
/MuonEG/Run2016F-Nano02Apr2020-v1/NANOAOD	16002165 (13.6Gb)	3.1
/SingleElectron/Run2016F-Nano02Apr2020-v1/NANOAOD	70593532 (51.4Gb)	
/SingleMuon/Run2016F-Nano02Apr2020-v1/NANOAOD	65489554 (42.4Gb)	
Run 2016G		
/DoubleEG/Run2016G-Nano02Apr2020-v1/NANOAOD	78797031 (61.6Gb)	
/DoubleMuon/Run2016G-Nano02Apr2020-v1/NANOAOD	45235604 (34.2Gb)	
/MuonEG/Run2016G-Nano02Apr2020-v1/NANOAOD	33854612 (29.0Gb)	7.6
/SingleElectron/Run2016G-Nano02Apr2020-v1/NANOAOD	153363109 (109.2Gb)	
/SingleMuon/Run2016G-Nano02Apr2020-v1/NANOAOD	149912248 (94.6Gb)	
Run 2016H		
/DoubleEG/Run2016H-Nano02Apr2020-v1/NANOAOD	85388734 (67.7Gb)	
/DoubleMuon/Run2016H-Nano02Apr2020-v1/NANOAOD	48912812 (37.3Gb)	
/MuonEG/Run2016H-Nano02Apr2020-v1/NANOAOD	29236516 (26.0Gb)	8.6
/SingleElectron/Run2016H-Nano02Apr2020-v1/NANOAOD	128854598 (93.8Gb)	
/SingleMuon/Run2016H-Nano02Apr2020-v1/NANOAOD	174035164 (110.2Gb)	

2017 data samples

Dataset	Events (size)	$\mathcal{L}$ [fb^{-1}]
Run 2017B		
/DoubleEG/Run2017B-Nano02Apr2020-v1/NANOAOD	58088760 (46.6Gb)	
/DoubleMuon/Run2017B-Nano02Apr2020-v1/NANOAOD	14501767 (10.8Gb)	
/SingleElectron/Run2017B-Nano02Apr2020-v1/NANOAOD	60537490 (42.2Gb)	4.8
/SingleMuon/Run2017B-Nano02Apr2020-v1/NANOAOD	136300266 (86.2Gb)	
/MuonEG/Run2017B-Nano02Apr2020-v1/NANOAOD	4453465 (4.1Gb)	
Run 2017C		
/DoubleEG/Run2017C-Nano02Apr2020-v1/NANOAOD	65181125 (53.8Gb)	
/DoubleMuon/Run2017C-Nano02Apr2020-v1/NANOAOD	49636525 (39.5Gb)	
/SingleElectron/Run2017C-Nano02Apr2020-v1/NANOAOD	136637888 (102.5Gb)	9.7
/SingleMuon/Run2017C-Nano02Apr2020-v1/NANOAOD	165652756 (109.5Gb)	
/MuonEG/Run2017C-Nano02Apr2020-v1/NANOAOD	15595214 (15.0Gb)	
Run 2017D		
/DoubleEG/Run2017D-Nano02Apr2020-v1/NANOAOD	25911432 (21.6Gb)	
/DoubleMuon/Run2017D-Nano02Apr2020-v1/NANOAOD	23075733 (18.6Gb)	
/SingleElectron/Run2017D-Nano02Apr2020-v1/NANOAOD	51526710 (38.5Gb)	4.2
/SingleMuon/Run2017D-Nano02Apr2020-v1/NANOAOD	70361660 (47.2Gb)	
/MuonEG/Run2017D-Nano02Apr2020-v1/NANOAOD	9164365 (8.9Gb)	
Run 2017E		
/DoubleEG/Run2017E-Nano02Apr2020-v1/NANOAOD	56233597 (49.8Gb)	
/DoubleMuon/Run2017E-Nano02Apr2020-v1/NANOAOD	51589091 (44.4Gb)	
/SingleElectron/Run2017E-Nano02Apr2020-v1/NANOAOD	102121689 (81.3Gb)	9.3
/SingleMuon/Run2017E-Nano02Apr2020-v1/NANOAOD	154630534 (111.0Gb)	
/MuonEG/Run2017E-Nano02Apr2020-v1/NANOAOD	19043421 (19.2Gb)	
Run 2017F		
/DoubleEG/Run2017F-Nano02Apr2020-v1/NANOAOD	74307066 (67.1Gb)	
/DoubleMuon/Run2017F-Nano02Apr2020-v1/NANOAOD	79756560 (68.0Gb)	
/SingleElectron/Run2017F-Nano02Apr2020-v1/NANOAOD	128467223 (105.2Gb)	13.5
/SingleMuon/Run2017F-Nano02Apr2020-v1/NANOAOD	242135500 (178.3Gb)	
/MuonEG/Run2017F-Nano02Apr2020-v1/NANOAOD	25776363 (26.3Gb)	

2018 data samples

Dataset	Events (size)	$\mathcal{L}$ [fb^{-1}]
Run 2018A		
/DoubleMuon/Run2018A-Nano02Apr2020-v1/NANOAOD	75499908 (62.6Gb)	13.5
/EGamma/Run2018A-Nano02Apr2020-v1/NANOAOD	327843843 (261.8Gb)	
/SingleMuon/Run2018A-Nano02Apr2020-v1/NANOAOD	241608232 (167.7Gb)	
/MuonEG/Run2018A-Nano02Apr2020-v1/NANOAOD	32958503 (32.3Gb)	
Run 2018B		
/DoubleMuon/Run2018B-Nano02Apr2020-v1/NANOAOD	35057758 (28.3Gb)	6.8
/EGamma/Run2018B-Nano02Apr2020-v1/NANOAOD	153822427 (123.1Gb)	
/SingleMuon/Run2018B-Nano02Apr2020-v1/NANOAOD	119918017 (82.3Gb)	
/MuonEG/Run2018B-Nano02Apr2020-v1/NANOAOD	16211567 (15.8Gb)	
Run 2018C		
/DoubleMuon/Run2018C-Nano02Apr2020-v1/NANOAOD	34565869 (27.6Gb)	6.6
/EGamma/Run2018C-Nano02Apr2020-v1/NANOAOD	147827904 (119.2Gb)	
/SingleMuon/Run2018C-Nano02Apr2020-v1/NANOAOD	110032072 (75.7Gb)	
/MuonEG/Run2018C-Nano02Apr2020-v1/NANOAOD	15652198 (15.3Gb)	
Run 2018D		
/DoubleMuon/Run2018D-Nano02Apr2020_ver2-v1/NANOAOD	168605834 (128.6Gb)	32.0
/EGamma/Run2018D-Nano02Apr2020-v1/NANOAOD	751348648 (583.6Gb)	
/SingleMuon/Run2018D-Nano02Apr2020-v1/NANOAOD	513867253 (344.5Gb)	
/MuonEG/Run2018D-Nano02Apr2020_ver2-v1/NANOAOD	71961587 (68.6Gb)	

2016 MC samples

Process	Sample	Cross section [pb]
Drell-Yan	DYJetsToLL_M-10to50_TuneCUETP8M1_13TeV-madgraphMLM-pythia8 ($H_T < 70$ GeV)	18610.0
	DYJetsToLL_M-5to50_HT-70to100_TuneCUETP8M1_13TeV-madgraphMLM-pythia8	303.8
	DYJetsToLL_M-5to50_HT-100to200_TuneCUETP8M1_13TeV-madgraphMLM-pythia8	224.2
	DYJetsToLL_M-5to50_HT-200to400_TuneCUETP8M1_13TeV-madgraphMLM-pythia8	37.2
	DYJetsToLL_M-5to50_HT-400to600_TuneCUETP8M1_13TeV-madgraphMLM-pythia8	3.581
	DYJetsToLL_M-5to50_HT-600toInf_TuneCUETP8M1_13TeV-madgraphMLM-pythia8	1.124
	DYJetsToLL_M-50_TuneCUETP8M1_13TeV-madgraphMLM-pythia8 ($H_T < 70$ GeV)	6025.20
	DYJetsToLL_M-50_HT-70to100_TuneCUETP8M1_13TeV-madgraphMLM-pythia8	169.9
	DYJetsToLL_M-50_HT-100to200_TuneCUETP8M1_13TeV-madgraphMLM-pythia8	147.4
	DYJetsToLL_M-50_HT-200to400_TuneCUETP8M1_13TeV-madgraphMLM-pythia8	40.99
	DYJetsToLL_M-50_HT-400to600_TuneCUETP8M1_13TeV-madgraphMLM-pythia8	5.678
	DYJetsToLL_M-50_HT-600to800_TuneCUETP8M1_13TeV-madgraphMLM-pythia8	1.367
	DYJetsToLL_M-50_HT-800to1200_TuneCUETP8M1_13TeV-madgraphMLM-pythia8	0.6304
	DYJetsToLL_M-50_HT-1200to2500_TuneCUETP8M1_13TeV-madgraphMLM-pythia8	0.1514
	DYJetsToLL_M-50_HT-2500toInf_TuneCUETP8M1_13TeV-madgraphMLM-pythia8	0.003565
TTTo2L2Nu	TTTo2L2Nu_TuneCUETP8M2_ttHtranche3_13TeV-powheg-pythia8	87.310
Single top	ST_s-channel_4f_leptonDecays_13TeV-amcatnlo-pythia8_TuneCUETP8M1	3.360
	ST_t-channel_antitop_4f_inclusiveDecays_13TeV-powhegV2-madspin-pythia8_TuneCUETP8M1	80.95
	ST_t-channel_top_4f_inclusiveDecays_13TeV-powhegV2-madspin-pythia8_TuneCUETP8M1	136.02
	ST_tW_antitop_5f_inclusiveDecays_13TeV-powheg-pythia8_TuneCUETP8M1	35.60
	ST_tW_top_5f_inclusiveDecays_13TeV-powheg-pythia8_TuneCUETP8M1	35.60
ttV	TTWJetsToLNu_TuneCUETP8M1_13TeV-amcatnloFXFX-madspin-pythia8	0.2043
	ttZJets_13TeV_madgraphMLM-pythia8	0.7826
	TTZToLLNuNu_M-10_TuneCUETP8M1_13TeV-amcatnlo-pythia8	0.2529
WW	WWTo2L2Nu_13TeV-powheg	12.178
	WWJJToLNuLNu_EWK_noTop_13TeV-madgraph-pythia8	0.34520
	GluGluWWTo2L2Nu_MCFM_13TeV	0.5905
Vγ/Vγ*	WGToLNuG_TuneCUETP8M1_13TeV-madgraphMLM-pythia8	405.271
	ZGTo2LG_TuneCUETP8M1_13TeV-amcatnloFXFX-pythia8	131.300
	WZTo3LNu_mllmin01_13TeV-powheg-pythia8	58.59
VZ	ZZTo2L2Nu_13TeV_powheg_pythia8	0.5640
	ZZTo2L2Q_13TeV_powheg_pythia8	3.22
	ZZTo4L_TuneCP5_13TeV_powheg_pythia8	1.212
	WZTo2L2Q_13TeV_amcatnloFXFX_madspin_pythia8	5.595
VVV	ZZZ_TuneCUETP8M1_13TeV-amcatnlo-pythia8	0.01398
	WZZ_TuneCUETP8M1_13TeV-amcatnlo-pythia8	0.05565
	WWZ_TuneCUETP8M1_13TeV-amcatnlo-pythia8	0.16510
	WWW_4F_TuneCUETP8M1_13TeV-amcatnlo-pythia8	0.18331
Non-Prompt	Data-driven (tight-to-loose method)	

2017 MC samples

Process	Sample	Cross section [pb]
Drell-Yan	DYJetsToLL_M-10to50_TuneCP5_13TeV-madgraphMLM-pythia8 ($H_T < 100$ GeV)	18610
	DYJetsToLL_M-4to50_HT-100to200_TuneCP5_13TeV-madgraphMLM-pythia8	204.0
	DYJetsToLL_M-4to50_HT-200to400_TuneCP5_13TeV-madgraphMLM-pythia8	54.39
	DYJetsToLL_M-4to50_HT-400to600_TuneCP5_13TeV-madgraphMLM-pythia8	5.697
	DYJetsToLL_M-4to50_HT-600toInf_TuneCP5_13TeV-madgraphMLM-pythia8	1.85
	DYJetsToLL_M-50_TuneCP5_13TeV-madgraphMLM-pythia8 ($H_T < 70$ GeV)	6189.39
	DYJetsToLL_M-50_HT-70to100_TuneCP5_13TeV-madgraphMLM-pythia8	169.9
	DYJetsToLL_M-50_HT-100to200_TuneCP5_13TeV-madgraphMLM-pythia8	161.1
	DYJetsToLL_M-50_HT-200to400_TuneCP5_13TeV-madgraphMLM-pythia8	48.66
	DYJetsToLL_M-50_HT-400to600_TuneCP5_13TeV-madgraphMLM-pythia8	6.968
	DYJetsToLL_M-50_HT-600to800_TuneCP5_13TeV-madgraphMLM-pythia8	1.743
	DYJetsToLL_M-50_HT-800to1200_TuneCP5_13TeV-madgraphMLM-pythia8	0.8052
	DYJetsToLL_M-50_HT-1200to2500_TuneCP5_13TeV-madgraphMLM-pythia8	0.1933
	DYJetsToLL_M-50_HT-2500toInf_TuneCP5_13TeV-madgraphMLM-pythia8	0.003468
TTTo2L2Nu	TTTo2L2Nu_TuneCP5_13TeV-powheg-pythia8	87.310
Single top	ST_s-channel_4f_leptonDecays_mtop1715_TuneCP5_PSweights_13TeV-amcatnlo-pythia8	3.360
	ST_t-channel_antitop_4f_inclusiveDecays_TuneCP5_13TeV-powhegV2-madspin-pythia8	80.95
	ST_t-channel_top_4f_inclusiveDecays_TuneCP5_13TeV-powhegV2-madspin-pythia8	136.02
	ST_tW_antitop_5f_inclusiveDecays_TuneCP5_13TeV-powheg-pythia8	35.60
	ST_tW_top_5f_inclusiveDecays_TuneCP5_13TeV-powheg-pythia8	35.60
ttV	ttWJets_TuneCP5_13TeV_madgraphMLM_pythia8	0.6105
	TTWJetsToLNu_TuneCP5_PSweights_13TeV-amcatnloFXFX-madspin-pythia8	0.2001
	ttZJets_TuneCP5_13TeV_madgraphMLM_pythia8	0.7826
	TTZToLLNuNu_M-10_TuneCP5_PSweights_13TeV-amcatnlo-pythia8	0.2529
WW	WWTo2L2Nu_NNPDF31_TuneCP5_PSweights_13TeV-powheg-pythia8	12.178
	WWJJToLNuLNu_EWK_noTop_TuneCP5_13TeV-madgraph-pythia8	0.34520
	GluGluToWWTo*_13TeV_MCFM701_pythia8	0.06387
Vγ/Vγ*	WGToLNuG_TuneCP5_13TeV-madgraphMLM-pythia8	405.271
	ZGToLLG_01J_5f_TuneCP5_13TeV-amcatnloFXFX-pythia8	58.83
	WZTo3LNu_mllmin01_NNPDF31_TuneCP5_13TeV_powheg_pythia8	58.59
VZ	ZZTo2L2Nu_13TeV_powheg_pythia8	0.5640
	ZZTo2L2Q_13TeV_amcatnloFXFX_madspin_pythia8	3.22
	ZZTo4L_TuneCP5_13TeV_powheg_pythia8	1.212
	WZTo2L2Q_13TeV_amcatnloFXFX_madspin_pythia8	5.595
VVV	ZZZ_TuneCP5_13TeV-amcatnlo-pythia8	0.01398
	WZZ_TuneCP5_13TeV-amcatnlo-pythia8	0.05565
	WWZ_4F_TuneCP5_13TeV-amcatnlo-pythia8	0.16510
	WWW_4F_TuneCP5_13TeV-amcatnlo-pythia8	0.18331
Non-Prompt	Data-driven (tight-to-loose method)	

2018 MC samples

Process	Sample	Cross section [pb]
Drell-Yan	DYJetsToLL_M-10to50_TuneCP5_13TeV-madgraphMLM-pythia8 ($H_T < 100$ GeV)	18610.0
	DYJetsToLL_M-4to50_HT-100to200_TuneCP5_PSweights_13TeV-madgraphMLM-pythia8	204.0
	DYJetsToLL_M-4to50_HT-200to400_TuneCP5_PSweights_13TeV-madgraphMLM-pythia8	54.39
	DYJetsToLL_M-4to50_HT-400to600_TuneCP5_PSweights_13TeV-madgraphMLM-pythia8	5.697
	DYJetsToLL_M-4to50_HT-600toInf_TuneCP5_PSWeights_13TeV-madgraphMLM-pythia8	1.85
	DYJetsToLL_M-50_TuneCP5_13TeV-amcatnloFXFX-pythia8 ($H_T < 70$ GeV)	6189.39
	DYJetsToLL_M-50_HT-70to100_TuneCP5_PSweights_13TeV-madgraphMLM-pythia8	169.9
	DYJetsToLL_M-50_HT-100to200_TuneCP5_PSweights_13TeV-madgraphMLM-pythia8	161.1
	DYJetsToLL_M-50_HT-200to400_TuneCP5_PSweights_13TeV-madgraphMLM-pythia8	48.66
	DYJetsToLL_M-50_HT-400to600_TuneCP5_PSweights_13TeV-madgraphMLM-pythia8	6.968
	DYJetsToLL_M-50_HT-600to800_TuneCP5_PSweights_13TeV-madgraphMLM-pythia8	1.743
	DYJetsToLL_M-50_HT-800to1200_TuneCP5_PSweights_13TeV-madgraphMLM-pythia8	0.8052
	DYJetsToLL_M-50_HT-1200to2500_TuneCP5_PSweights_13TeV-madgraphMLM-pythia8	0.1933
	DYJetsToLL_M-50_HT-2500toInf_TuneCP5_PSweights_13TeV-madgraphMLM-pythia8	0.003468
TTTo2L2Nu	TTTo2L2Nu_TuneCP5_13TeV-powheg-pythia8	87.310
Single top	ST_s-channel_4f_leptonDecays_TuneCP5_13TeV-madgraph-pythia8	3.360
	ST_t-channel_antitop_4f_InclusiveDecays_TuneCP5_13TeV-powheg-madspin-pythia8	80.95
	ST_t-channel_top_4f_InclusiveDecays_TuneCP5_13TeV-powheg-madspin-pythia8	136.02
	ST_tW_antitop_5f_inclusiveDecays_TuneCP5_13TeV-powheg-pythia8	35.60
	ST_tW_top_5f_inclusiveDecays_TuneCP5_13TeV-powheg-pythia8	35.60
ttV	ttWJets_TuneCP5_13TeV_madgraphMLM_pythia8	0.6105
	TTWJetsToLNu_TuneCP5_13TeV-amcatnloFXFX-madspin-pythia8	0.2043
	ttZJets_TuneCP5_13TeV_madgraphMLM_pythia8	0.7826
	TTZToLLNuNu_M-10_TuneCP5_13TeV-amcatnlo-pythia8	0.2529
WW	WWTo2L2Nu_NNPDF31_TuneCP5_13TeV-powheg-pythia8	12.178
	WWJJToLNuLNu_EWK_TuneCP5_13TeV-madgraph-pythia8	0.4286
	GluGluToWWTo*_TuneCP5_13TeV_MCFM701_pythia8	0.06387
Vγ/Vγ*	WGToLNuG_TuneCP5_13TeV-madgraphMLM-pythia8	405.271
	ZGToLLG_01J_5f_TuneCP5_13TeV-amcatnloFXFX-pythia8	131.300
	WZTo3LNu_mllmin01_NNPDF31_TuneCP5_13TeV_powheg_pythia8	58.59
VZ	ZZTo2L2Nu_TuneCP5_13TeV_powheg_pythia8	0.5640
	ZZTo2L2Q_13TeV_amcatnloFXFX_madspin_pythia8	3.22
	ZZTo4L_TuneCP5_13TeV_powheg_pythia8	1.212
	WZTo2L2Q_13TeV_amcatnloFXFX_madspin_pythia8	5.595
VVV	ZZZ_TuneCP5_13TeV-amcatnlo-pythia8	0.01398
	WZZ_TuneCP5_13TeV-amcatnlo-pythia8	0.05565
	WWZ_TuneCP5_13TeV-amcatnlo-pythia8	0.16510
	WWW_4F_TuneCP5_13TeV-amcatnlo-pythia8	0.18331
Non-Prompt	Data-driven (tight-to-loose method)	

$t/\bar{t}$+DM signal samples

Mass point	Cross-section [pb]
Scalar mediators	
DMscalar_Dilepton_top_tWChan_Mchi1_Mphi10	$4.959 \cdot 10^{-2}$
DMscalar_Dilepton_top_tWChan_Mchi1_Mphi20	$3.235 \cdot 10^{-2}$
DMscalar_Dilepton_top_tWChan_Mchi1_Mphi50	$1.323 \cdot 10^{-2}$
DMscalar_Dilepton_top_tWChan_Mchi1_Mphi100	$5.633 \cdot 10^{-3}$
DMscalar_Dilepton_top_tWChan_Mchi1_Mphi150	$3.397 \cdot 10^{-3}$
DMscalar_Dilepton_top_tWChan_Mchi1_Mphi200	$2.359 \cdot 10^{-3}$
DMscalar_Dilepton_top_tWChan_Mchi1_Mphi250	$1.720 \cdot 10^{-3}$
DMscalar_Dilepton_top_tWChan_Mchi1_Mphi300	$1.328 \cdot 10^{-3}$
DMscalar_Dilepton_top_tWChan_Mchi1_Mphi350	$1.018 \cdot 10^{-3}$
DMscalar_Dilepton_top_tWChan_Mchi1_Mphi400	$6.717 \cdot 10^{-4}$
DMscalar_Dilepton_top_tWChan_Mchi1_Mphi450	$4.535 \cdot 10^{-4}$
DMscalar_Dilepton_top_tWChan_Mchi1_Mphi500	$3.206 \cdot 10^{-4}$
DMscalar_Dilepton_top_tWChan_Mchi1_Mphi1000	$3.045 \cdot 10^{-5}$
Pseudoscalar mediators	
DMpseudoscalar_Dilepton_top_tWChan_Mchi1_Mphi10	$6.151 \cdot 10^{-3}$
DMpseudoscalar_Dilepton_top_tWChan_Mchi1_Mphi20	$5.869 \cdot 10^{-3}$
DMpseudoscalar_Dilepton_top_tWChan_Mchi1_Mphi50	$4.946 \cdot 10^{-3}$
DMpseudoscalar_Dilepton_top_tWChan_Mchi1_Mphi100	$3.658 \cdot 10^{-3}$
DMpseudoscalar_Dilepton_top_tWChan_Mchi1_Mphi150	$2.754 \cdot 10^{-3}$
DMpseudoscalar_Dilepton_top_tWChan_Mchi1_Mphi200	$2.097 \cdot 10^{-3}$
DMpseudoscalar_Dilepton_top_tWChan_Mchi1_Mphi250	$1.616 \cdot 10^{-3}$
DMpseudoscalar_Dilepton_top_tWChan_Mchi1_Mphi300	$1.253 \cdot 10^{-3}$
DMpseudoscalar_Dilepton_top_tWChan_Mchi1_Mphi350	$7.851 \cdot 10^{-4}$
DMpseudoscalar_Dilepton_top_tWChan_Mchi1_Mphi400	$4.371 \cdot 10^{-4}$
DMpseudoscalar_Dilepton_top_tWChan_Mchi1_Mphi450	$3.095 \cdot 10^{-4}$
DMpseudoscalar_Dilepton_top_tWChan_Mchi1_Mphi500	$2.321 \cdot 10^{-4}$
DMpseudoscalar_Dilepton_top_tWChan_Mchi1_Mphi1000	$2.791 \cdot 10^{-5}$

$t\bar{t}$+DM signal samples

Mass point	Cross-section [pb]
Scalar mediators	
TTbarDMJets_Dilepton_scalar_LO_TuneCP5_13TeV-madgraph-mcatnlo-pythia8_mChi_1_mPhi_50	$3.405 \cdot 10^{-1}$
TTbarDMJets_Dilepton_scalar_LO_TuneCP5_13TeV-madgraph-mcatnlo-pythia8_mChi_1_mPhi_100	$8.027 \cdot 10^{-2}$
TTbarDMJets_Dilepton_scalar_LO_TuneCP5_13TeV-madgraph-mcatnlo-pythia8_mChi_1_mPhi_150	$2.673 \cdot 10^{-2}$
TTbarDMJets_Dilepton_scalar_LO_TuneCP5_13TeV-madgraph-mcatnlo-pythia8_mChi_1_mPhi_200	$1.158 \cdot 10^{-2}$
TTbarDMJets_Dilepton_scalar_LO_TuneCP5_13TeV-madgraph-mcatnlo-pythia8_mChi_1_mPhi_250	$6.020 \cdot 10^{-3}$
TTbarDMJets_Dilepton_scalar_LO_TuneCP5_13TeV-madgraph-mcatnlo-pythia8_mChi_1_mPhi_300	$3.579 \cdot 10^{-3}$
TTbarDMJets_Dilepton_scalar_LO_TuneCP5_13TeV-madgraph-mcatnlo-pythia8_mChi_1_mPhi_350	$2.376 \cdot 10^{-3}$
TTbarDMJets_Dilepton_scalar_LO_TuneCP5_13TeV-madgraph-mcatnlo-pythia8_mChi_1_mPhi_400	$1.443 \cdot 10^{-3}$
TTbarDMJets_Dilepton_scalar_LO_TuneCP5_13TeV-madgraph-mcatnlo-pythia8_mChi_1_mPhi_450	$9.025 \cdot 10^{-4}$
TTbarDMJets_Dilepton_scalar_LO_TuneCP5_13TeV-madgraph-mcatnlo-pythia8_mChi_1_mPhi_500	$6.204 \cdot 10^{-4}$
TTbarDMJets_Dilepton_scalar_LO_TuneCP5_13TeV-madgraph-mcatnlo-pythia8_mChi_20_mPhi_100	$7.993 \cdot 10^{-2}$
TTbarDMJets_Dilepton_scalar_LO_TuneCP5_13TeV-madgraph-mcatnlo-pythia8_mChi_30_mPhi_100	$8.052 \cdot 10^{-2}$
TTbarDMJets_Dilepton_scalar_LO_TuneCP5_13TeV-madgraph-mcatnlo-pythia8_mChi_40_mPhi_100	$8.147 \cdot 10^{-2}$
TTbarDMJets_Dilepton_scalar_LO_TuneCP5_13TeV-madgraph-mcatnlo-pythia8_mChi_45_mPhi_100	$8.319 \cdot 10^{-2}$
TTbarDMJets_Dilepton_scalar_LO_TuneCP5_13TeV-madgraph-mcatnlo-pythia8_mChi_49_mPhi_100	$8.304 \cdot 10^{-2}$
TTbarDMJets_Dilepton_scalar_LO_TuneCP5_13TeV-madgraph-mcatnlo-pythia8_mChi_51_mPhi_100	$9.735 \cdot 10^{-4}$
TTbarDMJets_Dilepton_scalar_LO_TuneCP5_13TeV-madgraph-mcatnlo-pythia8_mChi_55_mPhi_100	$4.835 \cdot 10^{-4}$
Pseudoscalar mediators	
TTbarDMJets_Dilepton_pseudoscalar_LO_TuneCP5_13TeV-madgraph-mcatnlo-pythia8_mChi_1_mPhi_50	$3.440 \cdot 10^{-2}$
TTbarDMJets_Dilepton_pseudoscalar_LO_TuneCP5_13TeV-madgraph-mcatnlo-pythia8_mChi_1_mPhi_100	$2.164 \cdot 10^{-2}$
TTbarDMJets_Dilepton_pseudoscalar_LO_TuneCP5_13TeV-madgraph-mcatnlo-pythia8_mChi_1_mPhi_150	$1.414 \cdot 10^{-2}$
TTbarDMJets_Dilepton_pseudoscalar_LO_TuneCP5_13TeV-madgraph-mcatnlo-pythia8_mChi_1_mPhi_200	$9.773 \cdot 10^{-3}$
TTbarDMJets_Dilepton_pseudoscalar_LO_TuneCP5_13TeV-madgraph-mcatnlo-pythia8_mChi_1_mPhi_250	$6.753 \cdot 10^{-3}$
TTbarDMJets_Dilepton_pseudoscalar_LO_TuneCP5_13TeV-madgraph-mcatnlo-pythia8_mChi_1_mPhi_300	$4.808 \cdot 10^{-3}$
TTbarDMJets_Dilepton_pseudoscalar_LO_TuneCP5_13TeV-madgraph-mcatnlo-pythia8_mChi_1_mPhi_350	$2.742 \cdot 10^{-3}$
TTbarDMJets_Dilepton_pseudoscalar_LO_TuneCP5_13TeV-madgraph-mcatnlo-pythia8_mChi_1_mPhi_400	$1.409 \cdot 10^{-3}$
TTbarDMJets_Dilepton_pseudoscalar_LO_TuneCP5_13TeV-madgraph-mcatnlo-pythia8_mChi_1_mPhi_450	$9.302 \cdot 10^{-4}$
TTbarDMJets_Dilepton_pseudoscalar_LO_TuneCP5_13TeV-madgraph-mcatnlo-pythia8_mChi_1_mPhi_500	$6.618 \cdot 10^{-4}$
TTbarDMJets_Dilepton_pseudoscalar_LO_TuneCP5_13TeV-madgraph-mcatnlo-pythia8_mChi_20_mPhi_100	$2.166 \cdot 10^{-2}$
TTbarDMJets_Dilepton_pseudoscalar_LO_TuneCP5_13TeV-madgraph-mcatnlo-pythia8_mChi_30_mPhi_100	$2.164 \cdot 10^{-2}$
TTbarDMJets_Dilepton_pseudoscalar_LO_TuneCP5_13TeV-madgraph-mcatnlo-pythia8_mChi_40_mPhi_100	$2.162 \cdot 10^{-2}$
TTbarDMJets_Dilepton_pseudoscalar_LO_TuneCP5_13TeV-madgraph-mcatnlo-pythia8_mChi_45_mPhi_100	$2.180 \cdot 10^{-2}$
TTbarDMJets_Dilepton_pseudoscalar_LO_TuneCP5_13TeV-madgraph-mcatnlo-pythia8_mChi_49_mPhi_100	$2.151 \cdot 10^{-2}$
TTbarDMJets_Dilepton_pseudoscalar_LO_TuneCP5_13TeV-madgraph-mcatnlo-pythia8_mChi_51_mPhi_100	$1.993 \cdot 10^{-3}$
TTbarDMJets_Dilepton_pseudoscalar_LO_TuneCP5_13TeV-madgraph-mcatnlo-pythia8_mChi_55_mPhi_100	$7.750 \cdot 10^{-4}$

Extension of the transverse mass m_T to cases when pairs of same flavor particles decay into one visible and one invisible particle, such as the double $W \to l\nu$ decay.

Here, 2 neutrinos contribute to the presence of MET and the individual contribution of each particle ($\not{\mathbf{p}}_{\mathbf{T_1}}$, $\not{\mathbf{p}}_{\mathbf{T_2}}$) to this missing energy cannot be inferred. M_{T2}^{ll} is defined as:

$$\begin{cases} M_{T2}^2 = \min\limits_{\not{\mathbf{p}}_{\mathbf{T_1}} + \not{\mathbf{p}}_{\mathbf{T_2}} = \not{\mathbf{p}}_{\mathbf{T}_{\text{tot}}}} \left(\max \left(m_T^2(\mathbf{p_{T_1}}, \not{\mathbf{p}}_{\mathbf{T_1}}), m_T^2(\mathbf{p_{T_2}}, \not{\mathbf{p}}_{\mathbf{T_2}}) \right) \right) \\ m_T^2(\mathbf{p_T}, \not{\mathbf{p}}_{\mathbf{T}}) = 4\ |\mathbf{p_T}||\not{\mathbf{p}}_{\mathbf{T}}|\ \sin^2\left(\frac{\alpha}{2}\right) \end{cases}$$

Different combinations ($\not{\mathbf{p}}_{\mathbf{T_1}}$, $\not{\mathbf{p}}_{\mathbf{T_2}}$) satisfying the condition $\not{\mathbf{p}}_{\mathbf{T_1}} + \not{\mathbf{p}}_{\mathbf{T_2}} = \not{\mathbf{p}}_{\mathbf{T}_{\text{tot}}}$ then need to be probed, keeping only the combination which results in the lowest possible value.

The $t\bar{t}$ process is expected to have an endpoint exactly at the mass of the W boson, while our eventual signal does not have this limitation because of the pair of dark matter particles produced.

Input variables correlation

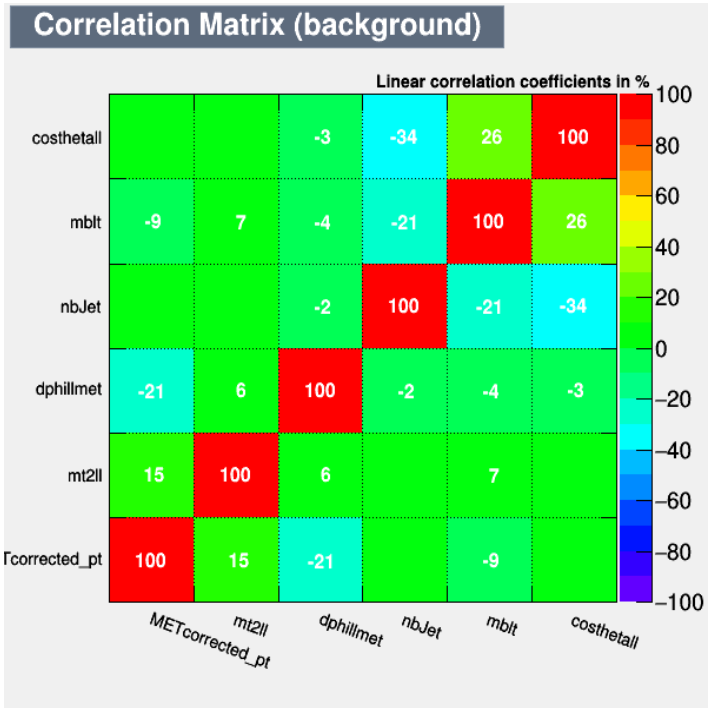

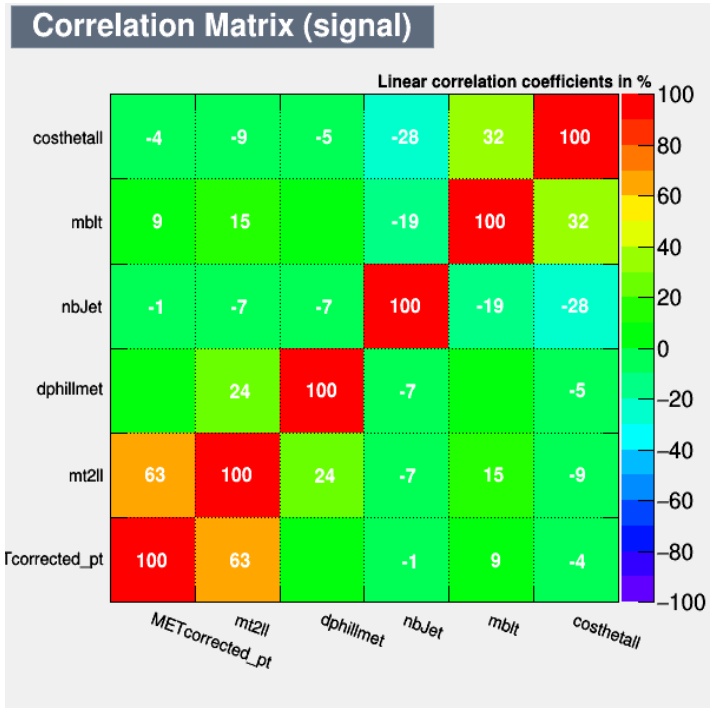

2016 discriminating variables

2016, // channel

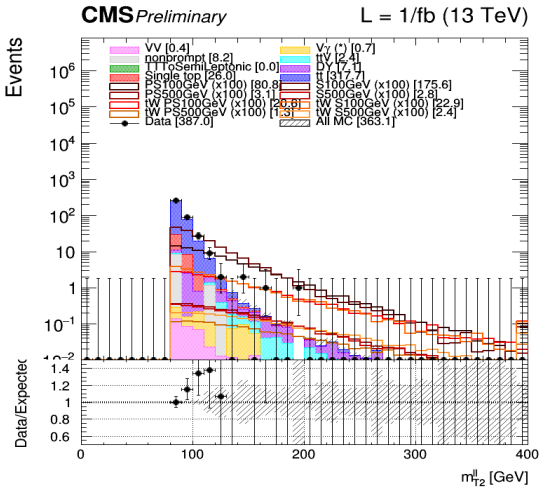

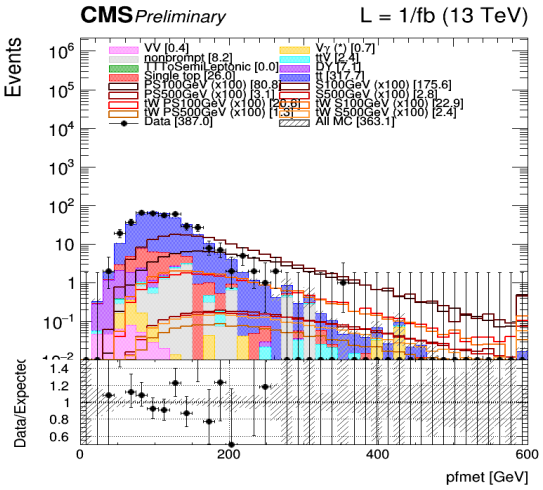

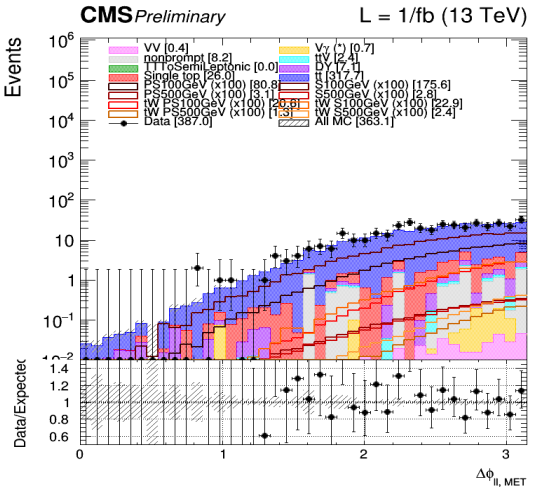

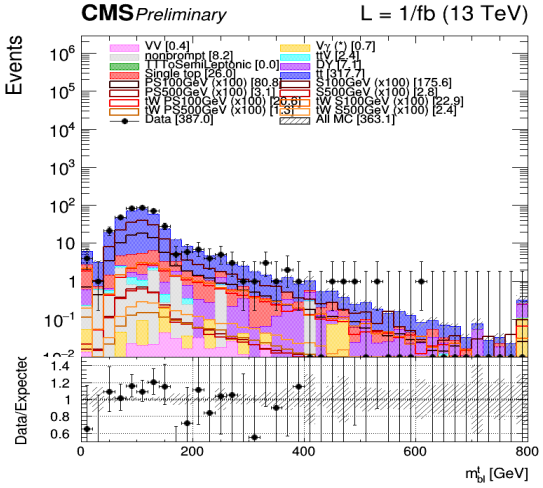

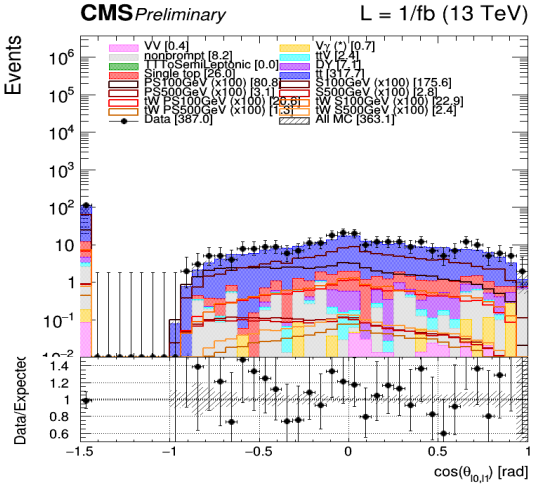

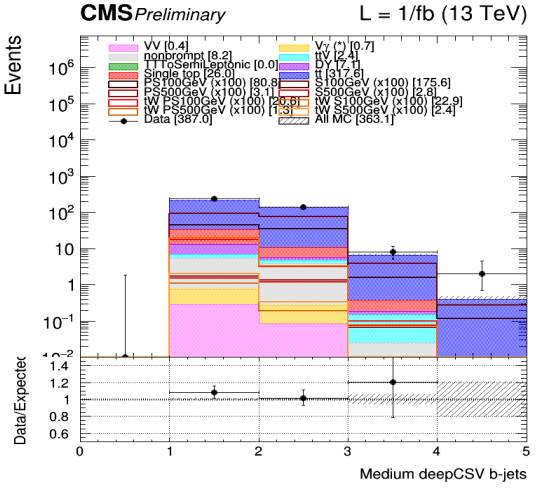

2017 discriminating variables

2017, // channel

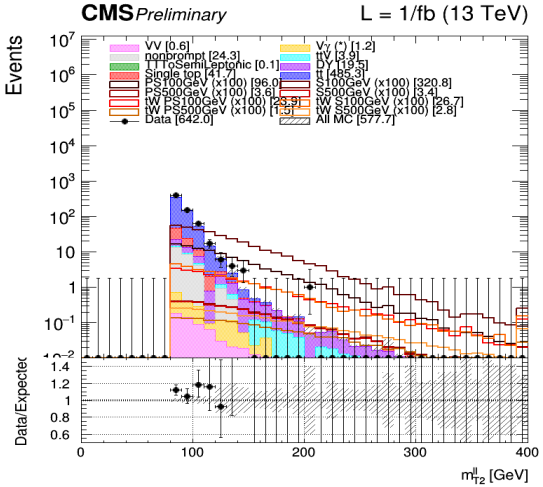

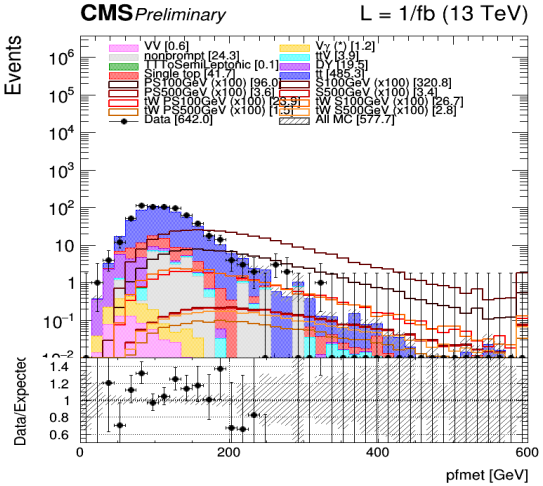

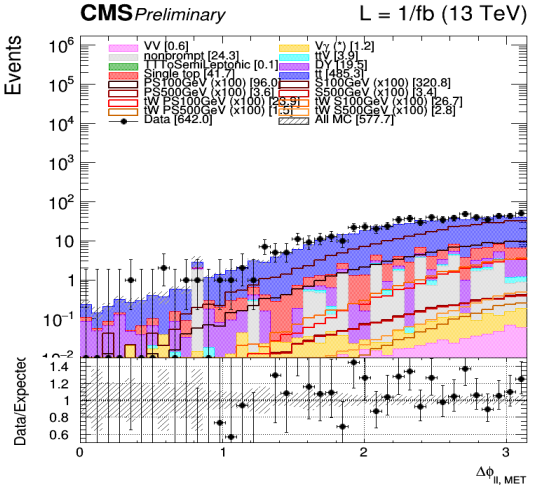

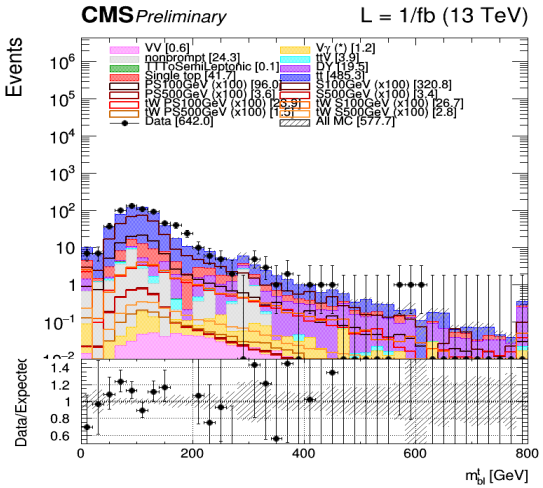

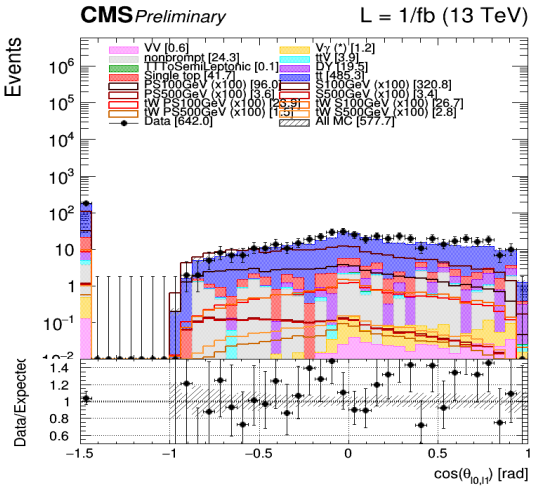

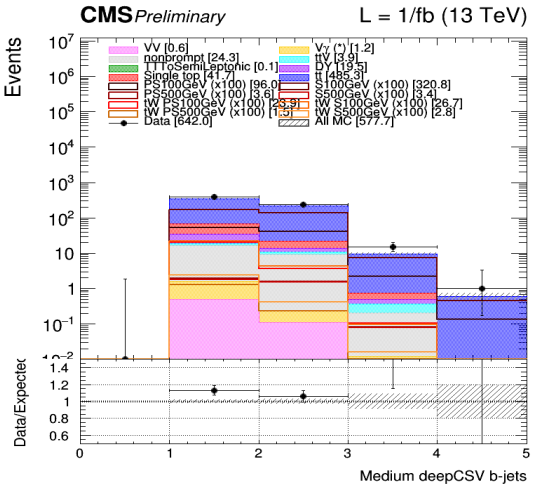

Blinded ANN output shape

Pseudoscalar 100 GeV output shape

2016

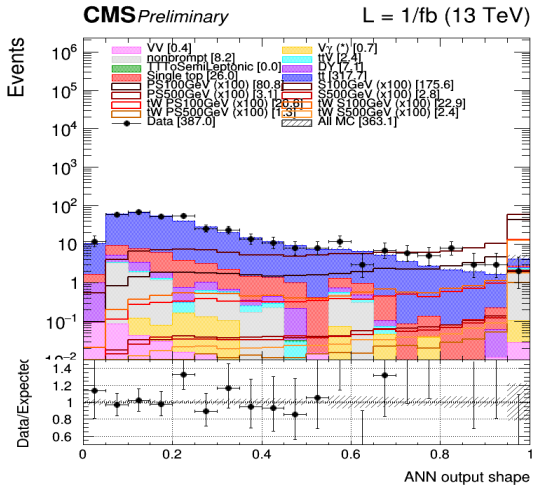

2017

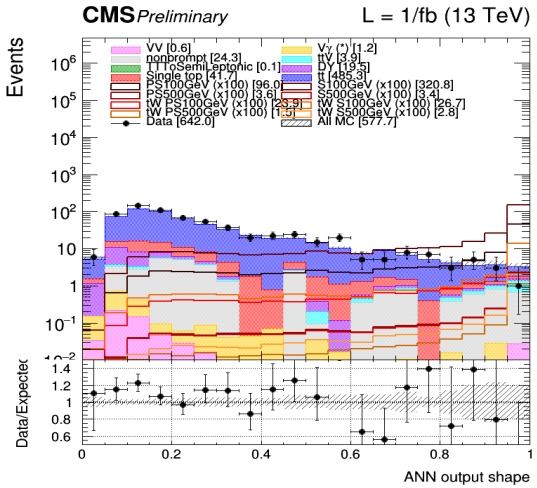

2018

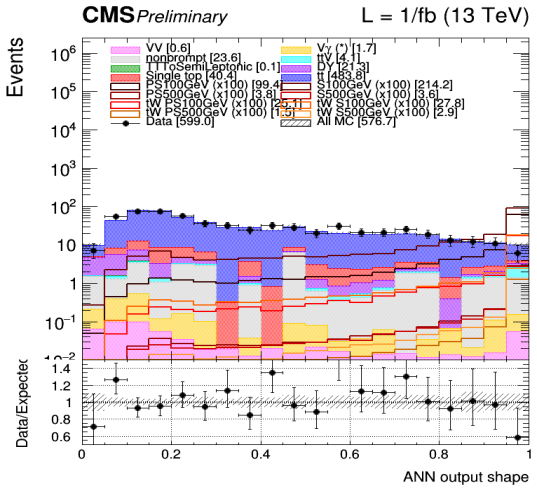

Pseudoscalar 500 GeV output shape

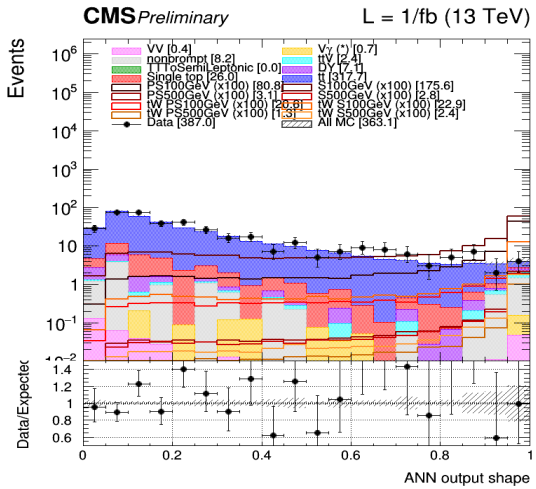

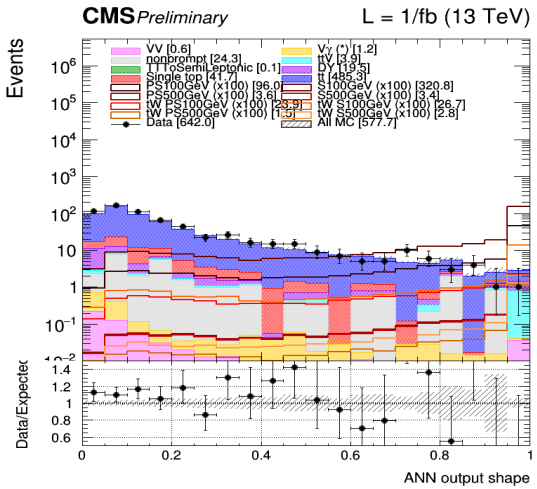

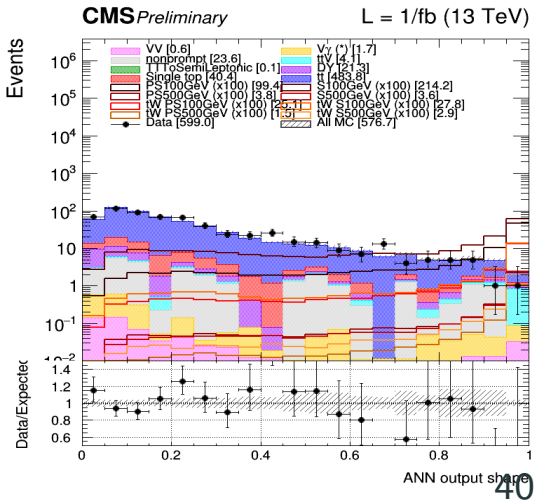

Scalar 100 GeV signal region

// channel

2016

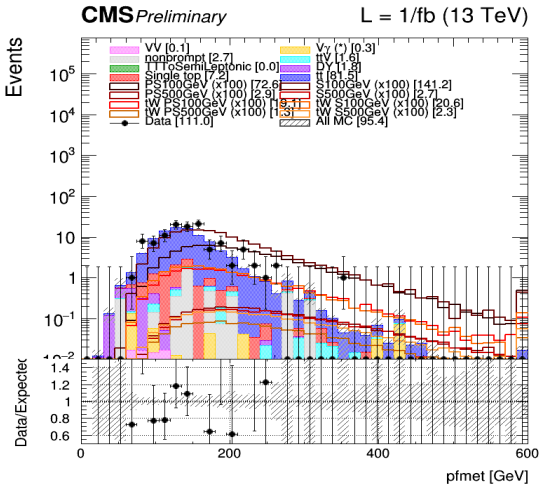

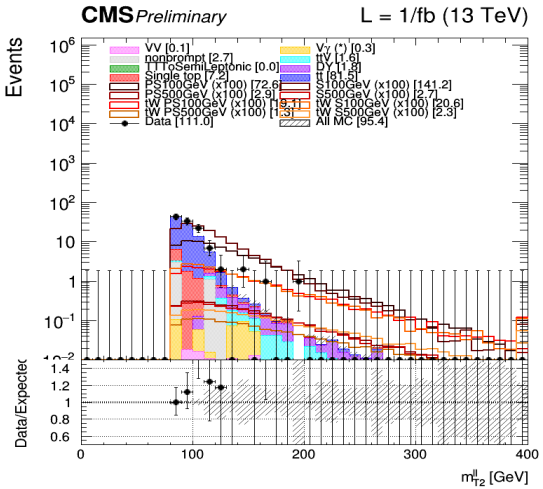

2017

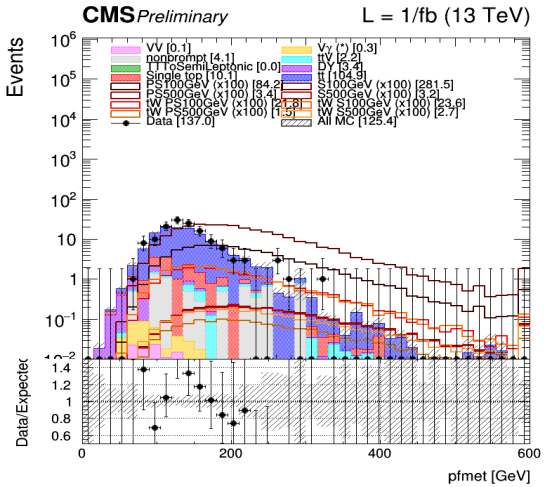

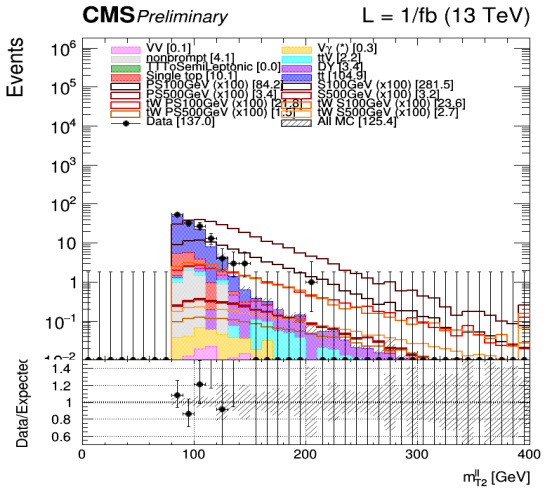

2018

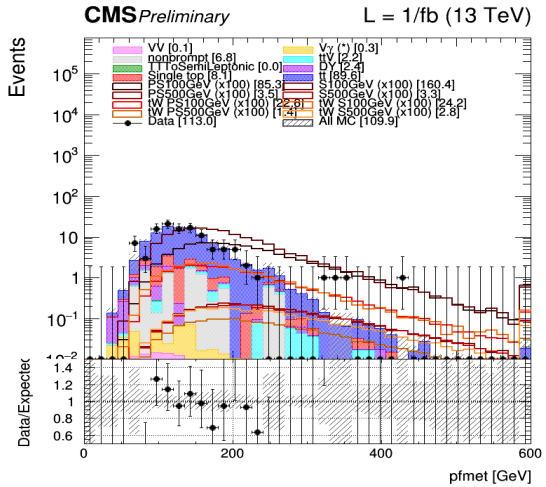

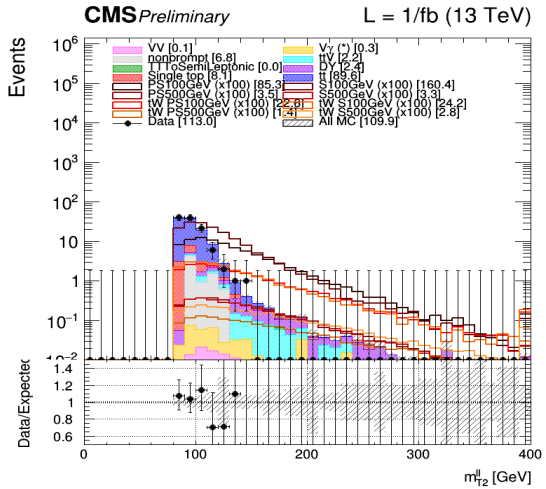

Scalar 500 GeV signal region

// channel

2016

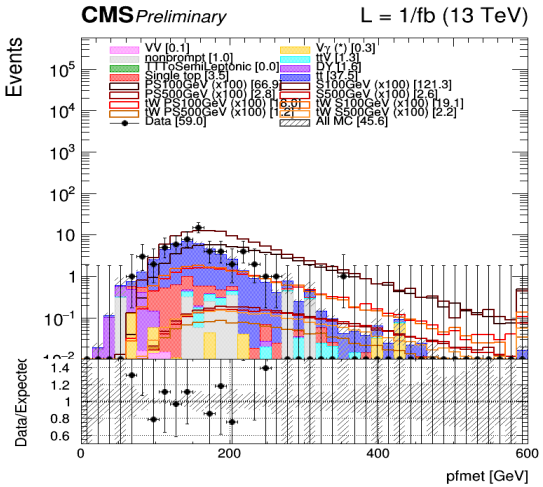

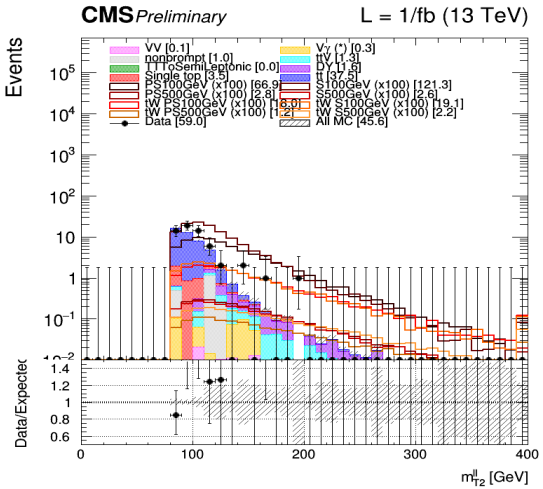

2017

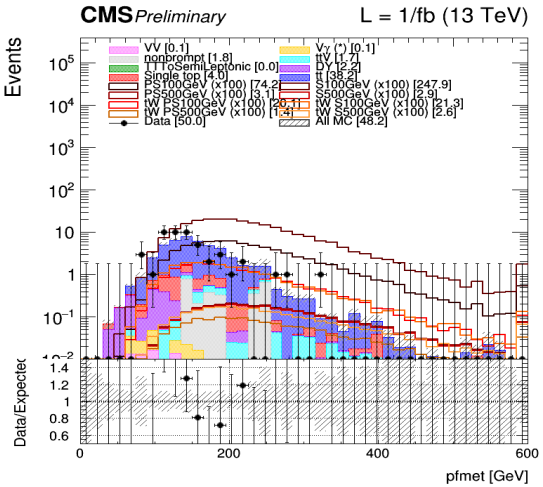

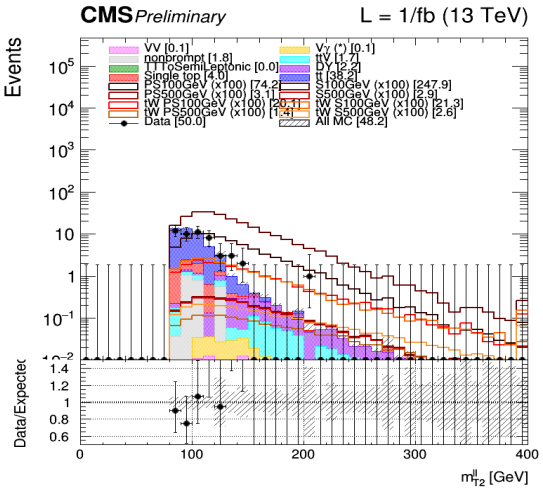

2018